Bias-corrected UKCP18 Convection-Permitting Model Projections for England

Qianyu Zha[1], Yi He[1], Timothy J. Osborn[2], Nicole Forstenhäusler[1]

[1]Tyndall Centre for Climate Change Research, School of Environmental Sciences, University of East Anglia, Norwich, NR4 7TJ, UK

[2]Climatic Research Unit, School of Environmental Sciences, University of East Anglia, Norwich, NR4 7TJ, UK

Correspondence to: Yi He (Yi.he@uea.ac.uk)

Abstract. The UKCP18 Convection-Permitting Model (CPM) provides the latest high-resolution climate projections for the UK. Compared with regional climate model projections, the CPM projections are more capable of simulating small-scale atmospheric convection particularly during extreme weather events such as intense rainfall and localis~~z~~ed storms. However, systematic biases still exist in these projections. To improve the reliability of these projections, bias correction is crucial. In this study, we apply and evaluate a quantile mapping (QM) bias correction method for UKCP18-CPM hourly precipitation (with diurnal correction) and daily temperature over England. We quantify how closely the bias corrected simulations align with observations relative to the raw simulations.~~we applied a quantile mapping (QM) method to correct hourly precipitation and daily temperature for four selected ensemble members (EM01, EM04, EM07, EM08) of the UKCP18-CPM for England.~~ The raw UKCP18-CPM simulations exhibit wet precipitation biases, particularly in northern England, with annual mean biases ranging from 4.6% to 18.3%, and cool temperature biases, with annual mean biases from -0.87 °C to 0.02 °C. Bias correction substantially improved agreement with observational datasets, increasing R^2 values for the 95th percentile of hourly precipitation from 0.80 –0.88 to 0.98 and achieving near-perfect alignment ($R^2 = 1$) for temperature extremes. Future projections for the 2070s indicate notable increases in annual maximum precipitation by 25.1 –39.1% and mean daily temperature by 3.1 °C to 4.5 °C, highlighting the potential for more intense climate-related events. Overall, the applied bias-correction method brings UKCP18-CPM simulations into closer agreement with observations for both mean behaviour and extremes, providing a more reliable basis for high-resolution impact modelling and assessments that require hourly precipitation forcing. ~~These results emphasize the effectiveness of bias correction in reducing model biases and improving the reliability of the CPM climate projections, thereby supporting more reliable future high-resolution climate and hydrological impact assessments in England.~~

1 Introduction

Global climate models (GCMs) are important tools for simulating present and future climates, widely used to project potential climate scenarios and assess the impacts of climate change on a global scale (IPCC, 2023a). However, GCMs often operate at relatively coarse spatial resolutions (ranging from 0.5° to 2.5°) and temporal scales (e.g., daily or monthly,

seasonally, or annually), which can limit their ability to accurately represent fine-scale regional climate variations (IPCC, 2023b; Keller et al., 2022; Tabari et al., 2021). This underscores the need for higher-resolution climate data to improve regional impact assessments. To address this, regional climate models (RCMs) are commonly employed to dynamically downscale GCM outputs, generating data with finer spatial resolutions (typically between 0.1° and 0.5°). RCMs provide several potential benefits over GCMs, such as the ability to better represent local topographical features, improve simulations of extreme weather events, and offer more refined regional climate projections, particularly in areas with complex terrain and climate variability (Chokkavarapu and Mandla, 2019; Kendon et al., 2010; Vichot-Llano et al., 2020). Convection-permitting models (CPMs) have become a valuable tool in short-range weather forecasting due to their enhanced ability to represent convective processes in detail, improve forecast accuracy, and capture localised high-impact rainfall that coarser models often miss (e.g., Done et al., 2004; Lean et al., 2008; Roberts and Lean, 2008; Weisman et al., 2008; Weusthoff et al., 2010). CPMs have also been widely applied in Europe (Berthou et al., 2020; Pichelli et al., 2021), Asia (Murata et al., 2017; Yun et al., 2020), and Africa (Kendon et al., 2019a; Maurer et al., 2017), as well as other regions (Trapp et al., 2011), to enhance the representation of convective processes and improve the accuracy of climate projections.

The UK Climate Projections 2018 (UKCP18) provide~~s~~ the latest generation of national climate projections for climate impact studies for the UK (Murphy et al., 2018). Several recent studies have employed the UKCP18-RCM 12 km regional perturbed parameter ensemble (PPE), which was released in November 2018, to assess the potential impacts of climate change. These applications include investigations into river and groundwater flow (Hannaford et al., 2023; Kay et al., 2023), extreme weather events (Hanlon et al., 2021), flood risks (Gudde et al., 2024), and droughts (Reyniers et al., 2023). In 2019, an additional UKCP18 toolkit was introduced, featuring the 2.2 km Convection-Permitting Model (UKCP18-CPM), which offers access to reliable climate information at local and hourly scales (Kendon et al., 2019b). ~~CPMs have become a valuable tool in short range weather forecasting due to their enhanced ability to represent convective processes in detail, improve forecast accuracy, and capture localized high impact rainfall that coarser models often miss (e.g. Done et al., 2004; Lean et al., 2008; Roberts and Lean, 2008; Weisman et al., 2008; Weusthoff et al., 2010). It has been widely applied in Europe (Berthou et al., 2020; Pichelli et al., 2021), Asia (Murata et al., 2017; Yun et al., 2020), and Africa (Kendon et al., 2019a; Maurer et al., 2017), as well as other regions (Trapp et al., 2011), to enhance the representation of convective processes and improve the accuracy of climate projections.~~

Despite their widespread use, climate model projections often show systematic biases relative to observations (Kotlarski et al., 2014; Vautard et al., 2021). For example, the UKCP18-RCM 12 km ensemble shows biases, including ~~-~~overestimation of winter precipitation, particularly in the mean and the 95th percentile of daily precipitation (representing heavy precipitation events) across most regions, and strong spatial variability in summer, with overestimations in the north and underestimations in the south (Reyniers et al., 2025). For temperature, the ensemble shows an overall cold bias at the annual scale in the mean and extremes. In winter, biases vary spatially and suggest overestimated variability, whereas in summer temperatures are more consistently underestimated across the UK ~~the ensemble generally underestimates values across the mean, cold, and hot tails of the distribution, with larger cold biases in winter, overestimated temperature variability during winter, and~~

underestimated summer temperatures, except for an overestimated urban heat island effect (Reyniers et al., 2025). Building on the UKCP18-RCM, the UKCP18-CPM offers improvements, though notable issues persist. In winter, it remains too wet across most of the UK, while in summer it is too wet in the north and too dry in the southit shows spatial variability, being too wet in the north and too dry in the south (Kendon et al., 2021). For temperature, the UKCP18-CPM slightly reduces UK-wide biases in summer compared to the UKCP18-RCM, although it remains cooler in the far north and exhibits minimal differences elsewhere (Kendon et al., 2021). In winter, the UKCP18-CPM introduces colder biases, particularly in northern regions, which are linked to its improved representation of snow processes, leading to greater snow accumulation and cooler temperatures (Kendon et al., 2021).

These biases, if left uncorrected, can severely affect the accuracy of climate impact assessments in sectors such as hydrology, ecology, and agriculture. The non-linear responses of impact models to these biases can amplify errors in projections, underscoring the importance of applying bias correction (BC) before using climate data in impact studies. In this paper, we use the term bias correction (BC) following common usage in the climate impact literature. However, these methods do not remove model biases in a physical sense; rather, they statistically adjust model outputs to better match an observational reference over a calibration period. We adopt this interpretation when discussing our results. Various BC methods, such as statistical downscaling, linear scaling, local intensity scaling, histogram equalizing, rank matching, and quantile mapping (QM), have been developed and evaluated (Gutmann et al., 2014; Maraun et al., 2019; Teutschbein and Seibert, 2012). Amongst these, QM has emerged as a particularly effective approach (Lafon et al., 2013; Shah et al., 2024; Themeßl et al., 2011), not only adjusting the mean but also correcting standard deviations and percentiles, making it suitable for temperature and precipitation adjustments in climate impact studies (Fang et al., 2015; Themeßl et al., 2012; Wilcke et al., 2013). For example, Cannon et al. (2015) evaluated the QM for bias correction of GCM precipitation outputs, emphasizing its effectiveness in adjusting mean values and precipitation extremes, while Sangelantoni et al. (2019) demonstrated its applicability for RCM temperature and precipitation corrections over Central Italy, particularly for seasonal and extreme climate variables.

In the UK, the UKCP18-RCM ensemble dataset has been widely used and bias-corrected for applications such as river flow, flood risk, and drought assessments (Hannaford et al., 2023; Robinson et al., 2023; Smith et al., 2025). In contrast, bias correction of the UKCP18-CPM ensemble remains limited. Kay and Brown (2023) applied a simple monthly scaling method to correct daily UKCP18-CPM precipitation data from the ensemble member 01 (EM01) against observations and kept temperature data uncorrected. However, this monthly scaling applied a uniform adjustment to all daily precipitation values within each month. It corrects monthly means but does not explicitly adjust the within-month distribution (e.g., quantiles and extremes)the scaling method applies a uniform adjustment across all precipitation values and cannot account for the distributions. As a result, it may not accurately correct biases in extreme precipitation events. It also fails to correct the diurnal cycle of precipitation, which is a key feature of high-resolution climate models (Bannister et al., 2019; Scaff et al., 2019). This is consistent with Faghih et al. (2022), who compared two bias-corrected time series using a multivariate quantile mapping method, both with and without correction of the diurnal cycle, and found that bias correction of the diurnal

cycle for sub-daily precipitation is preferable. Moreover, bias correction of sub-daily variables from CPMs is rare, largely due to two main challenges: (1) the substantial computational and memory demands associated with processing sub-daily data from high-resolution climate models, and (2) the relative scarcity of hourly observational datasets compared to daily observations, which poses challenges for the evaluation and correction of sub-daily variables from CPMs.

This study leverages a 1 km resolution gridded hourly observation-based rainfall dataset (CEH-GEAR1hr) for bias correcting the UKCP18-CPM hourly precipitation data. The CEH-GEAR1hr dataset (Lewis et al., 2022)~~.~~ integrates data from over 1,900 quality-controlled rainfall gauges over Great Britain, providing highly accurate precipitation measurements and enabling more robust sub-daily evaluation and bias correction of precipitation timing and intensity~~precise hydrological simulations by allowing detailed analysis of rainfall patterns on an hourly basis~~. For temperature, there is currently no observation-based hourly temperature dataset across the UK. Therefore, bias correction was performed on the UKCP18-CPM daily temperature using the Met Office's 1 km daily HadUK-Grid dataset (Hollis et al., 2019; Met Office et al., 2022) ~~compared two bias-corrected time series using a multivariate quantile mapping method, both with and without correction of the diurnal cycle, and found that bias correction of the diurnal cycle for sub-daily precipitation and temperature is preferable~~. Building on the findings of Faghih et al. (2022), we address a remaining gap: diurnal-cycle-aware bias correction is still rarely implemented and systematically evaluated for sub-daily precipitation in convection-permitting climate simulations, despite its importance for impact models that are sensitive to rainfall timing and intensity. The contribution of this paper is therefore application-driven evaluation in a CPM sub-daily setting, providing evidence on whether incorporating diurnal structure within quantile mapping improves (i) conventional climatological statistics and (ii) more challenging characteristics, including the diurnal cycle and sub-daily extremes.

The purpose of this paper is to present and assess a bias-correction method for UKCP18-CPM hourly precipitation and to quantify how closely the bias-adjusted UKCP18-CPM simulations align with observations relative to the raw simulations. ~~In this study, w~~We bias-corrected and evaluated the hourly precipitation and daily temperature variables from the UKCP18-CPM for England using the quantile mapping (QM) method. The UKCP18-CPM (Kendon et al., 2019b) consists of a 12-member convection-permitting model ensemble, which is nested within a 12-member RCM perturbed parameter ensemble (PPE), and further nested within a 12-member GCM PPE. Due to storage and computational constraints, we referenced the CHESS-SCAPE dataset (Robinson et al., 2023) and selected four ensemble members for this study (Sect. 2.3.1 Choice of sub-ensemble), including the default configuration ~~(~~EM01~~)~~ (also the driest member), the wettest members (EM04 and EM07), and a moderate member (EM08).~~and the driest member, the wettest members (EM04 and EM07), and a more moderate member (EM08).~~ The bias-corrected dataset features a high spatial resolution of 1 km, with hourly precipitation and daily temperature data. Specifically, we address the following research questions:

1. What biases are contained in the UKCP18-CPM simulations?
2. Can the QM bias correction method successfully correct errors in simple and more challenging metrics?
3. What climatic changes do the UKCP18-CPM ensemble members broadly project for England?

Addressing these questions is crucial for understanding and improving the applicability of UKCP18-CPM data in climate impact assessments.

2 Study area, data and methods

2.1 Study area

This study focuses on England (Fig. 1), with the primary aim of assessing the bias-correction method. Catchment boundaries are obtained from 249 catchments in the National River Flow Archive (NRFA) and are used only to define the analysis mask (i.e., to select the 1 km grid cells processed). Appendix A. Table A1 lists the NRFA IDs of the 249 catchments used to define the analysis mask in this study. No hydrological modelling or catchment-scale simulation is performed. The processed HadUK-Grid cells within this mask are displayed in Fig. 1 by their centre points. Given computational and storage constraints, restricting the analysis to grid cells within these catchments provides a practical and geographically coherent subset for the study. The catchments were selected based on the availability of complete gauged records for December 1990 to November 2000, overlapping with both the CEH-GEAR1hr observational dataset and the UKCP18-CPM baseline period (see Sect. 2.2.2; hereafter referred to as the reference period), and on minimal anthropogenic influence. Bias correction was applied independently at the grid-cell level to UKCP18-CPM precipitation and temperature for 62,488 1 km grid cells. Across the processed grid cells, the mean annual precipitation is approximately 2.64 mm d^{-1}, and the mean annual temperature is around 9.3 °C, based on the CEH-GEAR1hr and HadUK-Grid datasets, respectively.~~This study focuses on 249 catchments in England (Figure 1; catchment IDs are listed in Table A1 in Appendix A), selected from the CAMELS-GB dataset (Coxon et al., 2020). The catchments were chosen based on the availability of complete gauged data during the period from December 1990 to November 2000 (overlapping with the CEH-GEAR1hr observational dataset and the UKCP18-CPM baseline period; as detailed in Sect. 2.2.2 Observation-based datasets hereafter 'reference period') and minimal influence from anthropogenic activities, providing a basis for assessing natural hydrological responses. Bias correction was applied to the UKCP18-CPM precipitation and temperature data for 62,488 grid points at a 1 km resolution. The mean annual precipitation across the selected grid points is approximately 2.64 mm/day, and the mean annual temperature is around 9.3 °C, calculated using the CEH-GEAR1hr and HadUK-Grid datasets, respectively.~~

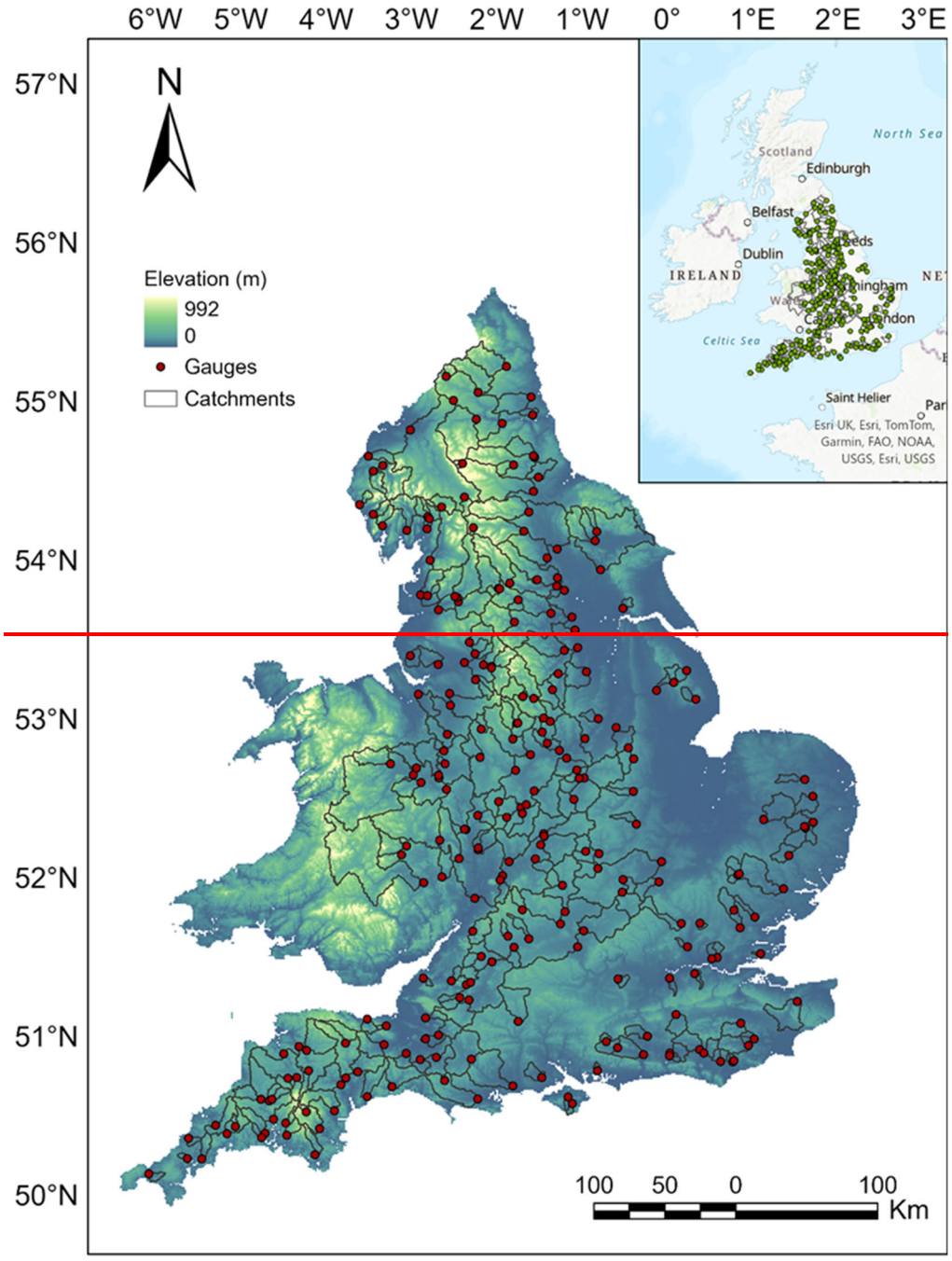
6°W
5°W
4°W
3°W
2°W
1°W
0°
1°E
2°E
3°E
57°N
56°N
55°N
54°N
53°N
52°N
51°N
50°N
N
Elevation (m)
992
0
Gauges
Catchments
North Sea
Scotland
Edinburgh
Belfast
Dublin
IRELAND
Celtic Sea
Saint Helier
Esri UK, Esri, TomTom, Garmin, FAO, NOAA, USGS, Esri, USGS
100
50
0
100
Km

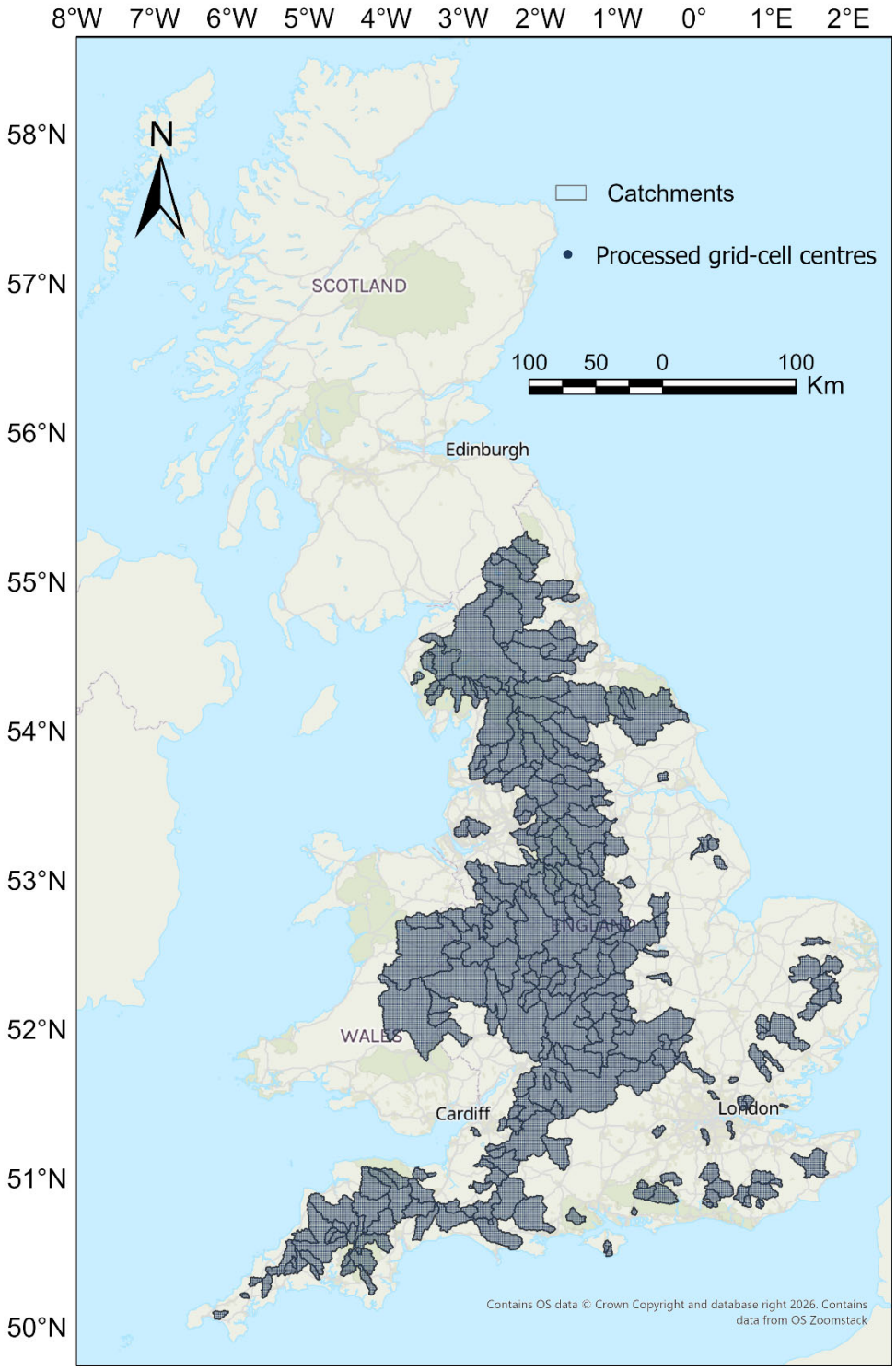
8°W
7°W
6°W
5°W
4°W
3°W
2°W
1°W
0°
1°E
2°E
58°N
57°N
56°N
55°N
54°N
53°N
52°N
51°N
50°N
N
Catchments
Processed grid-cell centres
SCOTLAND
100 50 0 100
Km
Edinburgh
ENGLAND
WALES
Cardiff
London
Contains OS data © Crown Copyright and database right 2026. Contains data from OS Zoomstack

Figure 1 Study domain in England. Catchment boundaries (249 catchments) are used only to define the analysis mask for grid-cell processing. The processed 1 km HadUK-Grid cells are displayed by their centre points.~~:~~

~~Location of the 249 selected catchments and their flow gauges in England overlapped on the elevation map.~~

2.2 Datasets

2.2.1 UKCP18 Convection-permitting model projections (UKCP18-CPM)

The UK Climate Projections 2018 (UKCP18) represent the latest set of national climate projections for the UK, offering a broad range of temporal coverage and spatial resolutions (Murphy et al., 2018). The land component of UKCP18 comprises three strands of information. Strand 1 updates the probabilistic predictions from UKCP09, providing a more comprehensive range of possible climate outcomes under specified emission scenarios. Strand 2 delivers a new set of global climate model (GCM) projections at approximately 60 km resolution, and it captures uncertainties in large-scale climate processes. Strand 3 is a perturbed parameter ensemble (PPE) of 12 regional climate model (RCM) projections derived from 12 of the 15 GC3.05-PPE simulations~~Strand 3 is a new perturbed parameter ensemble (PPE) of regional climate model (RCM) projections. It introduces a new ensemble consisting of 12 RCM simulations, which form a PPE of RCM variants derived from 12 out of the 15 GC3.05 PPE simulations~~ (Murphy et al., 2018). The projections from Strands 1, 2, and the 12 km RCM from Strand 3 were initially released in November 2018 (Murphy et al., 2018).

The UKCP18 convection-permitting model (UKCP18-CPM) projections are the UKCP18 Local (2.2 km) product (Kendon et al., 2019b), providing high-resolution climate information at ~2.2 km resolution and driven by the UKCP18 Regional (12 km) Strand 3 ensemble.~~, a new addition to the UKCP18 toolkit, provide high-resolution climate information at ~2.2 km resolution (Kendon et al., 2019b).~~ These projections explicitly capture small-scale physical processes and extreme weather events that are inadequately represented at coarser resolutions. CPM data are available on their native ~2.2 km rotated lat-lon grid and re-projected to a 5 km grid aligned with the Great Britain national grid (Met Office Hadley Centre, 2019). This study uses the re-projected 5 km CPM data for ensemble members 01 (EM01), 04 (EM04), 07 (EM07), and 08 (EM08) (see details in Sect. 2.3.1 Choice of sub-ensemble). These ensemble members adopt the standard RCM parameterizations (note that CPM-specific parameters are not adjusted between ensemble members). The 5 km dataset (Met Office Hadley Centre, 2019) was further re-gridded to the 1 km grid using the nearest neighbour interpolation method, assigning each 1 km grid cell the value of the corresponding 5 km grid cell in which it is located. This method was chosen to preserve the original value distribution and avoid artificial smoothing or interpolation artefacts that could arise from bilinear or higher-order methods, which is particularly important for preserving extreme values in precipitation and temperature relevant to impact studies. At the time of this study, the UKCP18-CPM data was available in three 20-year time slices: 1980-2000 (December 1980 to November 2000; baseline period), 2020-2040 (December 2020 to November 2040; 2030s), and 2060-2080 (December 2060 to November 2080; 2070s). The latter two are based on the high emissions scenario RCP8.5, which assumes high population growth and energy demand (Riahi et al., 2011). The data has 360 days for each meteorological year that begins on 1st December and ends on 30th November.

2.2.2 Observation-based datasets

As an observational reference for the evaluation and bias correction of UKCP18-CPM hourly precipitation, we used the 1 km resolution gridded hourly observation-based rainfall dataset, CEH-GEAR1hr (Lewis et al., 2022). This dataset is derived through the application of the nearest neighbour interpolation method to a national database of hourly rain gauge observations. The initial version of this dataset was published in 2019, covering the period from 1990 to 2014, and subsequently updated in 2022 (CEH-GEAR1hr v2) to extend the coverage to 1990-2016 (Hollis et al., 2019). For this study, we used CEH-GEAR1hr v2, which is available at the UKCEH Environmental Information Data Centre (Lewis et al., 2022). To evaluate the bias in the raw UKCP18-CPM projections compared to observations, we selected the overlapping portion of data from December 1990 to November 2000 (reference period).

To the best of our knowledge, there is currently no gridded, observation-based dataset in the UK that provides nationwide hourly temperature at high spatial resolution. Additionally, uncertainties exist when disaggregating temperature variables from daily to sub-daily scales, as indicated by previous studies on meteorological disaggregation processes (Breinl and Di Baldassarre, 2019). Therefore, this study focuses on the bias correction of the UKCP18-CPM daily temperature. For reference, the HadUK-Grid dataset (Hollis et al., 2019) is used. This dataset comprises gridded climate variables derived from the network of UK land surface observations and is produced by the Met Office Hadley Centre. It interpolates in situ observations to a regular grid, following methods developed in earlier datasets made available through the UK Climate Projections project (UKCIP02, UKCP09). The study uses Version 1.1.0.0 of the dataset, available on the CEDA Archive (Met Office et al., 2022).

2.3 Methods

2.3.1 Choice of sub-ensemble

As described in Sect. 2.2.1 UKCP18 Convection-permitting model projections (UKCP18-CPM), UKCP18 Strand 3 introduces a new ensemble consisting of 12 RCM simulations, which form a PPE of RCM variants derived from 12 out of the 15 GC3.05-PPE simulations (Murphy et al., 2018). Ensemble member 01 (EM01) serves as the standard configuration, generated without any parameter perturbations to provide a baseline reference for the ensemble. The other members are produced by varying specific parameters, such as cloud microphysics, aerosol forcing, ocean heat uptake, and atmospheric processes, to assess the model's response under diverse conditions (Sexton et al., 2021).

The UKCP18-CPM consists of 12 projections driven by the 12 km RCM ensemble. Due to computational and storage constraints, it was not practical to bias-correct the full CPM-PPE at 1 km hourly resolution. We therefore selected a subset of ensemble members for bias correction and implemented a parallel workflow on the University of East Anglia's high-performance computing (HPC) system to complete the processing within a reasonable time. ~~consists of 12 projections, driven by the 12 km RCM ensemble. Due to storage and computational constraints, bias-correcting the entire UKCP18 CPM PPE was impractical. Bias-correcting a single grid requires approximately 50 minutes on a single node of the~~

~~University of East Anglia's HPC cluster. With 62,488 grids within the 249 catchments for bias correction, multiple nodes were required for running parallel jobs on the cluster to ensure timely completion. Storage requirements further compounded these challenges, with pre-processed UKCP18 CPM hourly precipitation amounting to 576 GB, observational data 7.6 GB, and bias-corrected outputs 57 GB per ensemble member. The significant computational and storage demand limit this study to select a subset from the 12 ensemble members.~~ Four ensemble members were selected to represent the broad range of possible precipitation outcomes within the ensemble. This selection included the default configuration (EM01), as well as members representing the driest, wettest, and a more moderate response, focusing on variability in precipitation. It is reasonable to assume the CPM members inherit the larger scale patterns and projected changes from their parent RCMs members due to the one-way nesting approach applied within UKCP18. Therefore, we referred to the future precipitation changes projected by the UKCP18-RCM ensemble to guide the selection of CPM ensemble members. Table 1 summarises the percentage changes of precipitation in the 12 UKCP18-RCM ensemble members for the period 2060-2080 relative to 1980-2000.

Table 1. Percentage changes of precipitation in the 12 UKCP18-RCM ensemble members between the 1980-2000 and 2060-2080 (Robinson et al., 2023).

Ensemble member	Precipitation (%)				
	Annual	DJF	MAM	JJA	SON
01	−7	8	−2	−21	−17
04	5	21	4	−14	3
05	−2	8	1	−18	−4
06	−3	11	11	−40	−6
07	5	20	14	−27	5
08	1	15	9	−32	1
09	3	29	10	−33	−5
10	−2	13	7	−26	−8
11	−2	15	−5	−25	2
12	−3	13	−8	−17	−10
13	−5	23	−15	−38	−6
15	1	14	2	−25	4

*Ensemble members used for this study

We chose the following:

- **EM01** represents the default parameterisation of the climate model, chosen as a reference point. EM01 is the driest member, showing an overall decrease in annual precipitation, characterised by the smallest increase in winter (DJF) precipitation and the largest reduction in autumn (SON) precipitation. It has the largest decrease in annual precipitation, making it a suitable choice for representing scenarios with very dry conditions.

- **EM04** exhibits the largest increase in annual precipitation, with substantial growth during winter (DJF), alongside smaller increases in spring (MAM) and autumn (SON), and the smallest reduction in summer (JJA). It represents the upper limit of precipitation increase, which is crucial for assessing wet scenario impacts.
- **EM07** is similar to EM04 in terms of annual precipitation increase but with a different seasonal distribution. EM07 shows pronounced increases in spring (MAM) and autumn (SON) but a greater decrease in summer (JJA). It is thus used to represent a scenario with more extreme seasonal variability.
- **EM08** represents a moderate change in annual precipitation, lying near the middle range of all 12 ensemble members. It shows limited change in autumn (SON) precipitation, various increases in winter (DJF) and spring (MAM), and a moderate decrease in summer (JJA). This makes EM08 an appropriate choice to illustrate balanced seasonal changes.

These four ensemble members were selected to capture a wide range of precipitation responses, from the driest to the wettest scenarios. This approach ensures that the corrected dataset captures a wide spectrum of possible outcomes, offering a robust understanding of potential precipitation changes across different seasons. The ensemble mean presented in this study represents the mean of these four selected members.

2.3.2 Bias correction

Quantile Mapping (QM) is a widely used bias correction method designed to address systematic discrepancies (biases) in climate model outputs by aligning their distributions with observed data, thereby enhancing the reliability of regional impact assessments (Ayugi et al., 2020; Ngai et al., 2017; Reyniers et al., 2025; Tani and Gobiet, 2019). The QM method applies a statistical transformation to correct modelled values based on observed distributions. This transformation can be expressed as (Piani et al., 2010):

$$x^o = f(x^m) \quad \textbf{(1)}$$

Where x^o and x^m are the observed and modelled values, respectively, and $f(\,)$ is the transformation function. In practice, the transformation is achieved by aligning the cumulative distribution functions (CDFs) of modelled and observed data. It can be defined as:

$$x^o = F_{obs}^{-1}(F_{mod}(x^m)) \quad \textbf{(2)}$$

Where F_{mod} is CDF of the modelled value and F_{obs}^{-1} is the inverse of the observed CDF, also referred to as the quantile function. Therefore, QM effectively adjusts the CDFs of modelled climate variables to match the observed, thereby correcting not only the mean but also the variance and extreme values in the data (Cannon et al., 2015; Thrasher et al., 2012). Among the different variants of QM, the non-parametric variant, often referred to as empirical QM, adjusts modelled values using the empirical CDFs of the observed and modelled values, rather than assuming specific parametric distributions (e.g. Boé et al., 2007; Themeßl et al., 2011, 2012). The empirical CDFs are estimated using tables of empirical percentiles, with linear interpolation applied to approximate values falling between the percentiles (Boé et al., 2007). This makes empirical

QM particularly suitable for handling variables like temperature and precipitation, which frequently exhibit non-linear and heterogeneous behaviours (Gudmundsson et al., 2012). In this study, the empirical CDFs for observations and raw CPM are constructed using the baseline period, and the resulting mapping function is applied to the full CPM time series (3 20-year time slices).~~the empirical QM method was selected to perform bias correction on hourly precipitation and daily temperature data from the UKCP18 CPM.~~

As Reiter et al. (2018) pointed out, when applied to the full calibration period as a whole, QM can correct the overall distribution, but it does not correct errors in the annual cycle.~~QM can correct the distribution of the complete timeseries, but does not correct for errors in the annual cycle.~~ They reviewed different subsampling lengths for quantile mapping applications and found that subsampling improves the performance of bias correction for daily precipitation from climate models, with monthly timescales being optimal across all QM methods. Therefore, we applied empirical QM for both precipitation and temperature using monthly subsampling. For daily temperature,~~,~~ the data was first divided into 12 groups, one for each month, and empirical quantile mapping was applied to each group individually. For hourly precipitation, a single correction applied to all hours can miss the diurnal cycle. This may influence the reliability of climate model outputs, particularly in regional impact assessments involving small catchments that exhibit rapid hydrological responses to precipitation~~For hourly precipitation, additional steps were taken to address finer temporal variability. Applying a uniform correction across all hours may overlook the diurnal variability inherent in sub-daily precipitation data. Hourly precipitation often exhibits diurnal variability, leading to discrepancies between modelled and observed values that vary over the course of the day. These discrepancies can influence the reliability of climate model outputs, particularly in regional impact assessments involving small catchments that exhibit rapid hydrological responses to precipitation~~ (Ban et al., 2014; Dai et al., 1999). To account for temporal variability, we applied a diurnal quantile mapping (DBC) method for hourly precipitation, based on Faghih et al. (2022). The data for each month was further divided into 24 hourly groups, with a 3 h~~ hour~~ moving window used to compute the hourly data. This resulted in 24 unique correction factors, one for each hour of the day, to account for diurnal variability. Empirical QM was then applied to each hourly group. This approach enhances the representation of the diurnal cycle and improves the accuracy of bias correction for sub-daily precipitation. The QM method was implemented using the 'fitQmapQUANT' function from the qmap R package (version 1.0-4), developed by Lukas Gudmundsson (Gudmundsson et al., 2012). Key parameters were configured to enhance the accuracy of the correction: the argument ‘qstep’ was set to 100, following the findings of Lafon et al. (2013), who demonstrated that increasing the number of quantiles reduces errors, with 100 quantiles achieving optimal results. Additionally, ‘type’ was set to linear to specify the type of interpolation between quantiles.

3 Results

3.1 Bias of raw simulations

Figure 2a shows the spatial distribution of relative biases (%) in mean hourly precipitation in the raw UKCP18-CPM simulations compared with CEH-GEAR1hr for the reference period. Figure 2b shows the change in the number of hourly rainfall events exceeding 20 mm h^{-1} in UKCP18-CPM relative to CEH-GEAR1hr over the reference period. The 20 mm h^{-1} threshold is commonly used as an indicator of potential flash flood producing rainfall in the UK ~~Figure 2a shows the spatial distribution of precipitation biases (%) and the frequency of events exceeding 20 mm/hour in the UKCP18-CPM datasets for the reference period (December 1990 to November 2000), with rainfall events exceeding 20 mm/hour identified as causing flash floods in the UK~~ (e.g., Kendon et al., 2023). The figure includes data from four ensemble members (EM01, EM04, EM07, EM08) and the ensemble mean (EMean). The figure is structured into three rows representing different temporal scales: annual bias (ANN, top row), winter season bias (DJF: December, January, February, middle row), and summer season bias (JJA: June, July, August, bottom row). A positive bias (blue) indicates an overestimation of precipitation, leading to wetter conditions, while a negative bias (red) indicates an underestimation, resulting in drier conditions.

From a spatial perspective, the annual bias (ANN) shows a consistent pattern across the four ensemble members, with wetter biases in the north and drier biases in the south. This north–south contrast is clearer in seasonal results than in the annual mean.~~demonstrates a consistent pattern across the four ensemble members, showing a consistent tendency for wetter biases in the north and drier biases in the south, although the spatial differentiation between north and south is relatively moderate on an annual basis.~~ The numerical biases for the annual average range from 4.6% (EM07) to 18.3% (EM04), indicating an overall overestimation of precipitation throughout the year.

In the winter season (DJF), biases are overall higher than those observed annually, with values ranging from 20.4% (EM01) to 43.5% (EM08). This suggests that the UKCP18-CPM tends to overestimate precipitation during winter across all four ensemble members. Spatially, the north-south contrast persists, with the northern regions generally showing wetter biases compared to the southern regions, although this gradient is not as pronounced as in the summer months. The general increase in wet bias across England during DJF implies a systematic overestimation of winter precipitation by the model.

The summer season (JJA), however, reveals the most distinct spatial gradient among four ensemble members, with a clear north-wet and south-dry pattern visible across all of them. The biases during JJA range from -0.8% (EM08) to 31% (EM04).

The biases in the frequency of hourly events exceeding 20 mm~~/hour~~ h^{-1} (Figure 2b) are generally low, which indicates that the UKCP18-CPM captures the occurrence of extreme rainfall events reasonably well, particularly in winter.

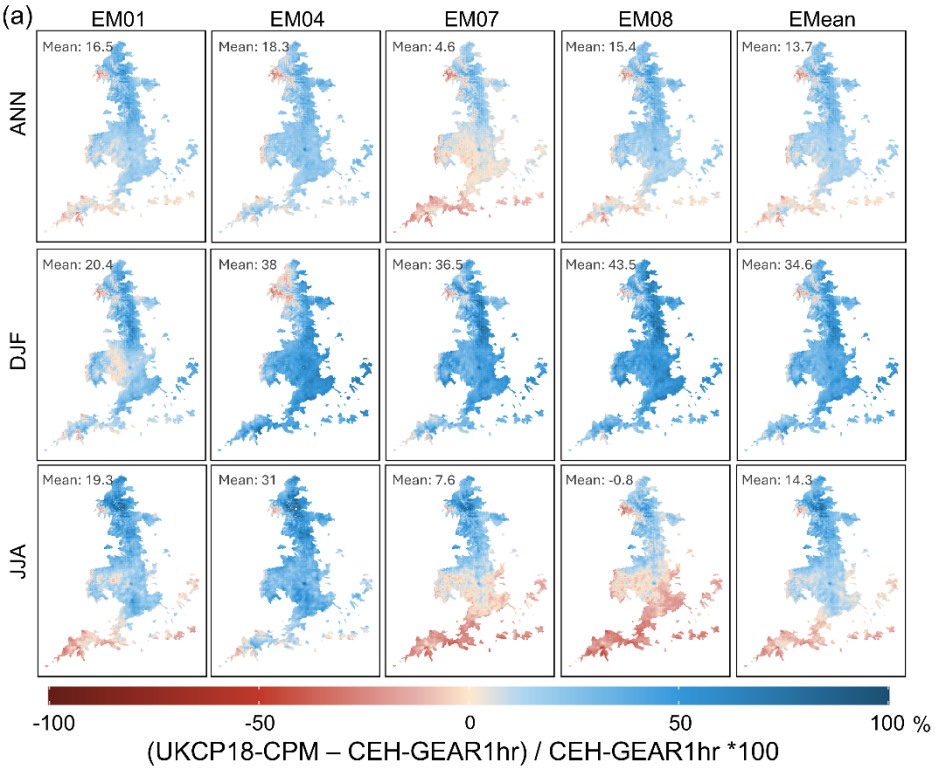
(a)
EM01
EM04
EM07
EM08
EMean
ANN
DJF
JJA
Mean: 16.5
Mean: 18.3
Mean: 4.6
Mean: 15.4
Mean: 13.7
Mean: 20.4
Mean: 38
Mean: 36.5
Mean: 43.5
Mean: 34.6
Mean: 19.3
Mean: 31
Mean: 7.6
Mean: -0.8
Mean: 14.3
-100
-50
0
50
100 %
(UKCP18-CPM – CEH-GEAR1hr) / CEH-GEAR1hr *100

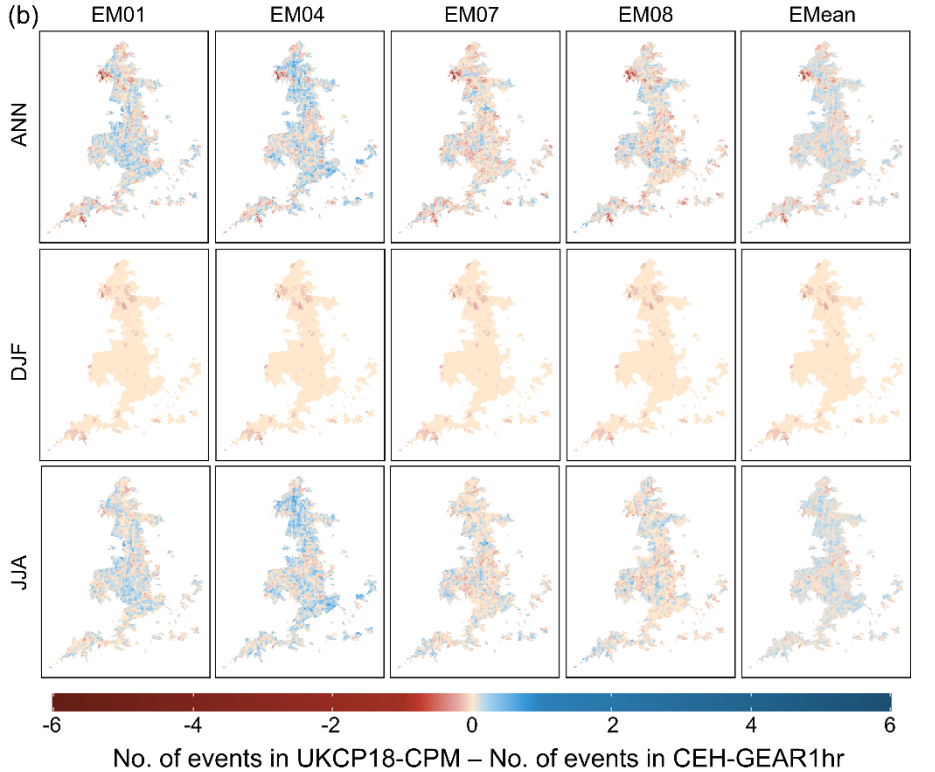
(b)
EM01
EM04
EM07
EM08
EMean
ANN
DJF
JJA
-6
-4
-2
0
2
4
6
No. of events in UKCP18-CPM – No. of events in CEH-GEAR1hr

330

Figure 2: **Spatial distribution of (a) relative biases (%) in mean hourly precipitation between UKCP18-CPM and CEH-GEAR1hr and (b) differences in the number of events exceeding 20 mm h^{-1} between UKCP18-CPM and CEH-GEAR1hr during the reference period across England. Rows represent annual (ANN), winter (DJF: December, January, February), and summer (JJA: June, July, August) results, while columns show individual ensemble members (EM01, EM04, EM07, EM08) and the ensemble mean (EMean). Blue indicates positive (wetter) biases and red indicates negative (drier) biases** ~~**Spatial distribution of (a) biases (%) of mean precipitation between UKCP18-CPM and CEH-GEAR1hr and (b) differences in the number of events exceeding 20 mm/hour between UKCP18-CPM and CEH-GEAR1hr for the reference period (December 1990 to November 2000) over England. Rows represent annual (ANN), winter (DJF: December, January, February), and summer (JJA: June, July, August) biases, while columns show individual ensemble members (EM01, EM04, EM07, EM08) and the ensemble mean (EMean)**~~**.**

Figure 3 shows the spatial distribution of biases in daily mean temperature from the UKCP18-CPM datasets for the reference period (December 1990 to November 2000). Each panel represents a different ensemble member (EM01, EM04, EM07, and EM08) and the ensemble mean (EMean). A positive bias (red) indicates an overestimation of temperature by the UKCP18-CPM, while a negative bias (blue) indicates an underestimation, compared to HadUK-Grid observations.

For the annual mean temperature (ANN), the ensemble members show a generally cool bias across England relative to HadUK-Grid, with mean biases ranging from -0.87 °C (EM04) to +0.02 °C (EM08). Three out of the four members have negative mean biases~~most ensemble members exhibit a cooler bias across England compared to the HadUK-Grid data, with biases ranging from -0.87 °C (EM04) to -0.42 °C (EM01). EM08, however, presents a slight warm bias of 0.02 °C, which contrasts with the cooler tendencies observed in other ensemble members~~. The spatial distribution of the annual temperature bias shows that the UKCP18-CPM generally predicts lower temperatures in the northern regions of England, while the southern regions show a tendency towards a warmer bias.

During winter (DJF), the temperature biases vary more clearly across ensemble members. EM04 exhibits a cold bias of -0.85 °C, whereas EM08 shows a warm bias of 0.46 °C, indicating marked inter-member differences in winter temperature bias.~~During the winter season (DJF), the biases are more pronounced, particularly in EM04, which shows a bias of -0.85 °C, indicating a substantial underestimation of winter temperatures compared to the observed dataset. EM08, conversely, has a warm bias of 0.46 °C, indicating an overestimation of winter temperatures.~~ The spatial distribution of winter biases is consistent with the annual trend, where the northern regions are generally colder in the model compared to the observed values, while some areas in the south exhibit a warmer bias. However, the contrast between ensemble members is evident, with EM07 showing only a slight positive bias (0.09 °C), indicating that the model's performance in simulating winter temperatures varies considerably between ensemble members.

For the summer season (JJA), all four ensemble members display a cooler bias. The biases range from -0.57 °C (EM07) to -0.08 °C (EM08), suggesting that the UKCP18-CPM tends to underestimate summer temperatures. The spatial pattern during JJA shows a clear north–south gradient, with stronger cooling biases in northern England and smaller biases in the south, a pattern that is consistent across all ensemble members.~~The spatial pattern during JJA shows a clear north-south gradient, with the north experiencing a stronger cooling bias compared to the south. This is consistent across all ensemble members, indicating a systematic underestimation of summer temperatures in the northern part of England, while the southern regions are closer to observed temperatures.~~

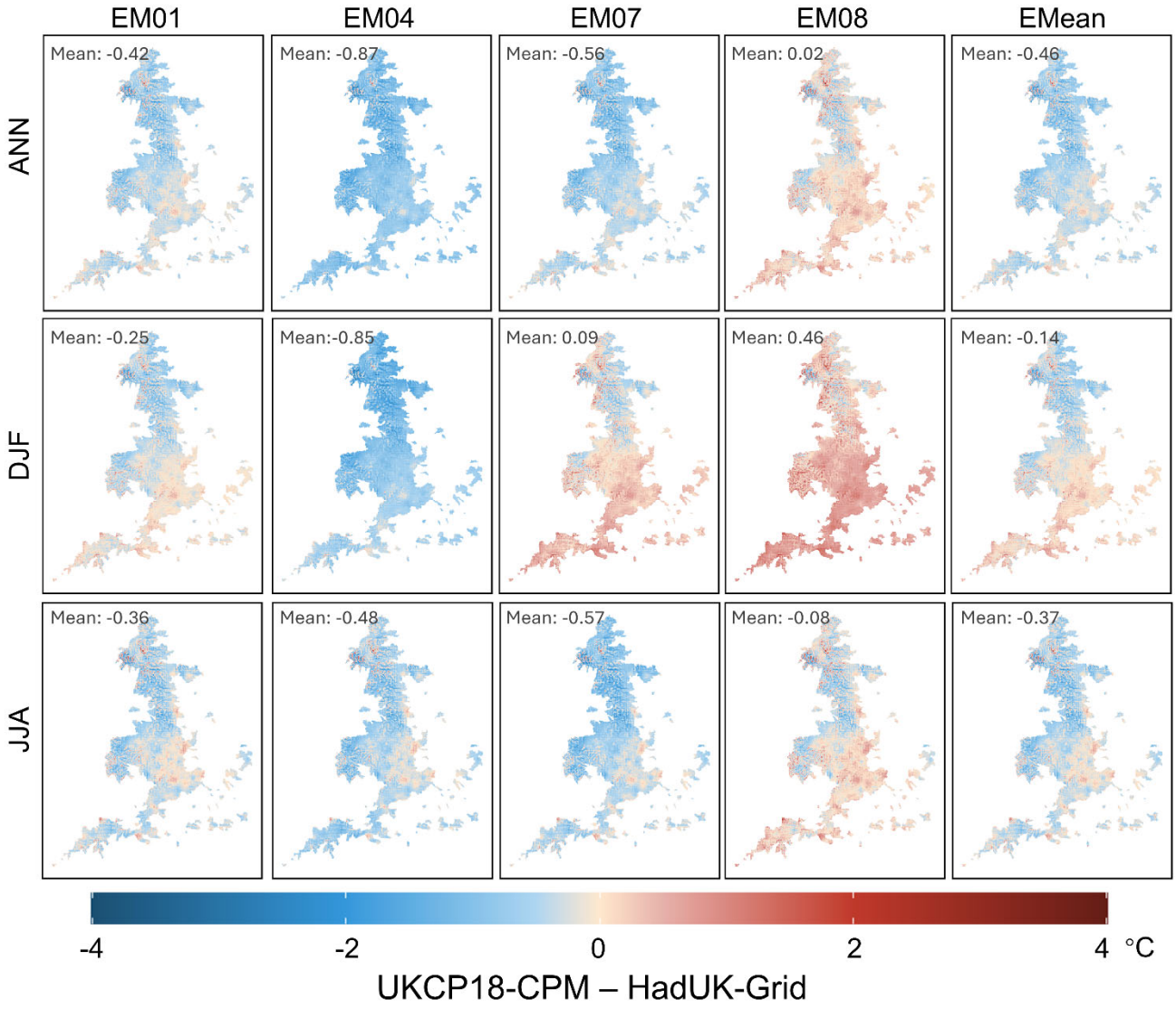

Figure 3: Temperature biases (°C) in UKCP18-CPM for the reference period (December 1990 to November 2000) over England. The panels show biases for each ensemble member (EM01, EM04, EM07, and EM08) and the ensemble mean (EMean). Rows represent different time scales: annual (ANN), winter (DJF: December, January, February), and summer (JJA: June, July, August). Red indicates positive (warmer) biases and blue indicates negative (cooler) biases.

3.2 Evaluation of bias correction

Figure 4 compares observed data with UKCP18-CPM simulations before and after bias correction for monthly precipitation (left, mm ~~/hour~~ h^{-1}) and temperature (right, °C) during the reference period (December 1990 to November 2000). Dashed lines represent raw (un-corrected) ensemble members (EM01, EM04, EM07, EM08), while solid lines indicate bias-corrected data (EM01BC, EM04BC, EM07BC, EM08BC). Observed values are marked with triangular symbols.

In the precipitation panel (left), the raw ensemble members deviate from observed values, particularly in winter and late summer. After bias correction, the solid lines align closely with observations, indicating effective reduction of errors. In the temperature panel (right), raw ensemble members also show noticeable deviations, especially during spring and winter. Bias correction improves the match, with the bias-corrected outputs closely following the observed temperatures throughout the year. Overall, Figure 4 shows that bias correction effectively aligns both precipitation and temperature simulations with observed data, reducing systematic discrepancies and improving the reliability of the UKCP18-CPM outputs.

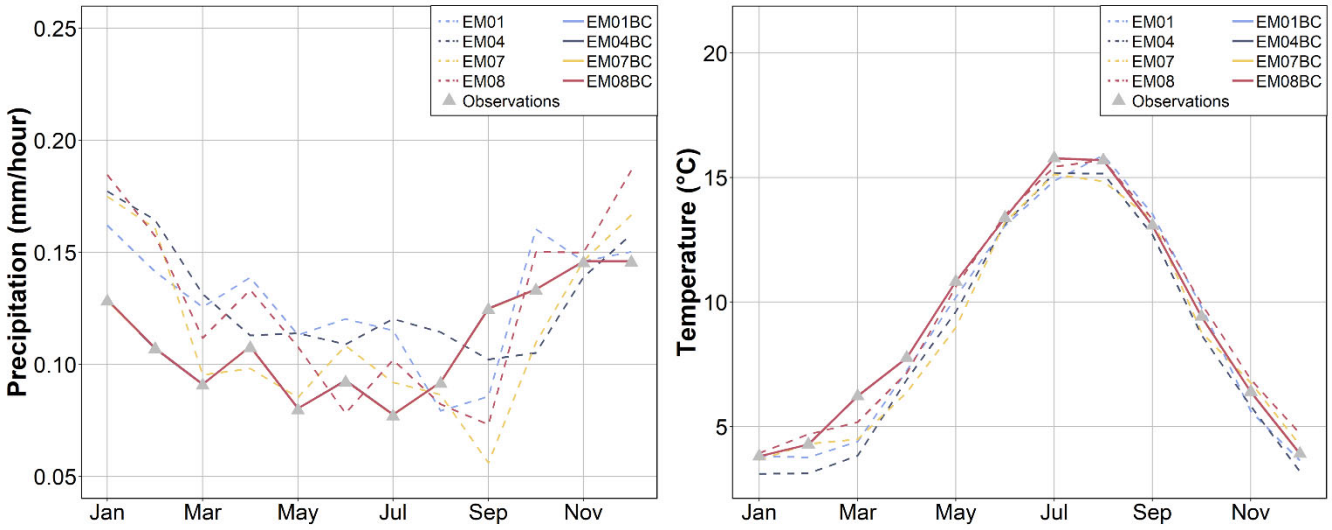

Figure 4: Comparison of monthly precipitation (left, mm/~~hour~~h^{-1}) and temperature (right, °C) between observed data and UKCP18-CPM simulations, before and after bias correction, for the reference period (December 1990 to November 2000). The blue, dark blue and yellow solid lines in both the precipitation and temperature panels lie underneath the red line~~The blue, dark bule and yellow solid lines underneath the red line in both precipitation and temperature panels~~.

Figure 5 demonstrates the effectiveness of the diurnal bias correction method (DBC) in adjusting the diurnal cycle of precipitation for the reference period (December 1990 to November 2000). The blue lines represent the UKCP18-CPM four ensemble members before bias correction, where the diurnal cycle exhibits noticeable discrepancies compared to CEH-GEAR1hr (depicted by the red line with circles). Specifically, the uncorrected ensemble tends to overestimate precipitation during most hours in winter, with the ensemble mean (darker blue line) consistently showing higher precipitation compared to the observations. In contrast, during summer and autumn, the uncorrected ensemble generally underestimates precipitation across most hours. After DBC, the yellow lines (UKCP18-CPM ensemble BC) illustrate significant improvements, with the corrected ensemble mean (thicker~~darker~~ yellow line) closely aligning with the observed diurnal cycle's temporal distribution and overall magnitude. Despite these improvements, some residual discrepancies remain, particularly in the smoother appearance of the bias-corrected results compared to CEH-GEAR1hr. These discrepancies are mainly related to the 3 h moving window used in the DBC process, which pools data from the target hour and its neighbouring hours to stabilise the hour-of-day correction.~~primarily due to the 3-hour moving window used during the DBC process, which was applied to filter out unreliable and unrealistic fluctuations in the observational data.~~

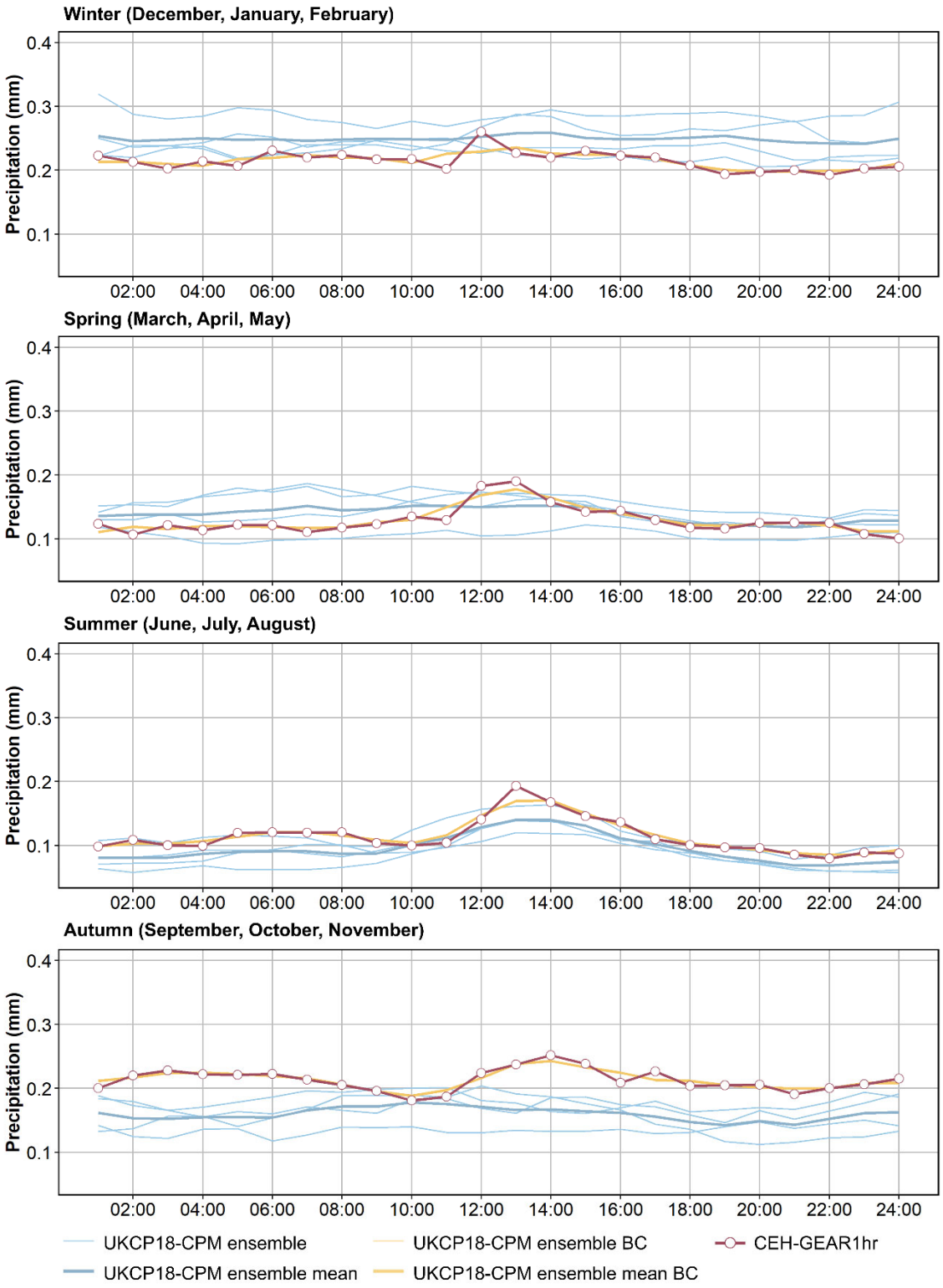
Winter (December, January, February)
Spring (March, April, May)
Summer (June, July, August)
Autumn (September, October, November)
Precipitation (mm)
0.4
0.3
0.2
0.1
02:00
04:00
06:00
08:00
10:00
12:00
14:00
16:00
18:00
20:00
22:00
24:00
UKCP18-CPM ensemble
UKCP18-CPM ensemble BC
CEH-GEAR1hr
UKCP18-CPM ensemble mean
UKCP18-CPM ensemble mean BC

Figure 5: Diurnal cycle of mean hourly precipitation before bias correction (blue lines: UKCP18-CPM ensemble) and after bias correction (yellow lines: UKCP18-CPM ensemble BC) for the reference period. The CEH-GEAR1hr (observations) are shown as a red solid line with circles. The ensemble mean before bias correction is shown as a darker blue line (UKCP18-CPM ensemble mean), and the bias-corrected ensemble mean is shown as a darker yellow line (UKCP18-CPM ensemble mean BC). The thin yellow lines (individual members) are overlain by the thick yellow line (ensemble mean), as the diurnal cycles are similar across the four members.~~Diurnal cycle of precipitation before bias correction (blue lines: UKCP18-CPM ensemble) and after bias correction (yellow lines: UKCP18-CPM ensemble BC) for the reference period (December 1990 to November 2000). The CHE-GEAR1hr (observations) are shown as a red solid line with circles. The ensemble mean before bias correction is shown as a darker blue line (UKCP18-CPM ensemble mean), and the bias-corrected ensemble mean is shown as a darker yellow line (UKCP18-CPM ensemble mean BC).~~

To evaluate the bias-corrected precipitation extremes in the UKCP18-CPM dataset, the 95th percentile (P_{95}) of hourly precipitation for the reference period was calculated and compared to that of the CEH-GEAR1hr dataset (observations), as shown in Figure 6. Here, the percentile refers to the percentile value itself (i.e., the threshold value), rather than to all values above or below that threshold. The top row displays scatter plots of the P_{95} values from UKCP18-CPM against CEH-GEAR1hr for each ensemble member, both before (light blue) and after (dark blue) bias correction. The closer the points are to the x=y line, the better the correspondence between the UKCP18-CPM and observations, indicating higher model accuracy. Initially, the raw UKCP18-CPM data shows a fair correlation with the observations, with gradients between 0.89 to 1 and R^2 values ranging from 0.80 to 0.88, indicating some discrepancies in capturing extreme values. After bias correction, the R^2 values improve to 0.98, demonstrating a much closer fit to observations. Before bias correction, the higher P95 values (>2 mm/h) are largely underestimated by the CPM, which is shown as horizontal scatter of dots. Bias correction can correct these values closer to the observed values although still slightly underestimated. The bottom row presents violin plots of the P_{95} distributions for observations (black), raw UKCP18-CPM (light blue), and bias-corrected UKCP18-CPM (dark blue). These plots indicate that the bias correction not only adjusts the mean values but also better aligns the overall distribution of extreme precipitation with the observed data, reducing discrepancies in spread and central tendency.

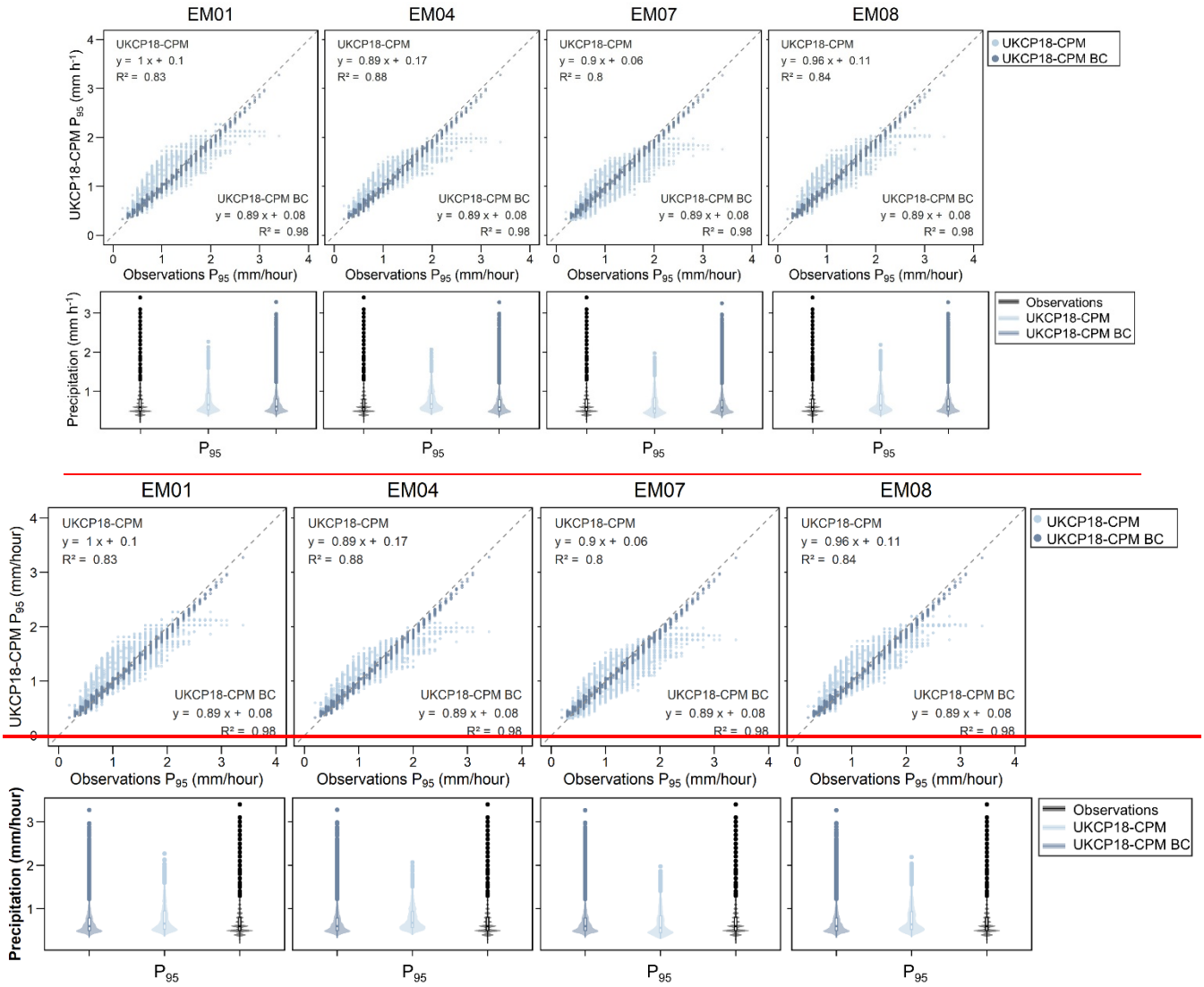

Figure 6: Comparison of 95th percentile (P_{95}) hourly precipitation values for the reference period. The top row shows scatter plots of UKCP18-CPM P_{95} values for each ensemble member, plotted against CEH-GEAR1hr observations for each 1 km grid, with raw (light blue) and bias-corrected (dark blue) data. The bottom row presents violin plots of P_{95} values for observations (black), raw UKCP18-CPM (light blue), and bias-corrected (dark blue) data. ~~Comparison of 95th percentile (P_{95}) hourly precipitation values for the reference period (December 1990 to November 2000). The top row shows scatter plots of UKCP18-CPM P_{95} values for each ensemble member, plotted against CEH-GEAR1hr observations for each 1km grid, with raw (light blue) and bias-corrected (dark blue) data. The bottom row presents violin plots of P_{95} values for observations (black), raw UKCP18-CPM (light blue), and bias-corrected (dark blue) data.~~

Temperature extremes were evaluated by comparing the 95th (T_{95}) and 5th (T_5) percentiles of daily mean temperature in UKCP18-CPM with HadUK-Grid for the reference period. Figure 7 shows grid-cell scatter plots (T_{95} in the top row and T_5 in the bottom row) for each ensemble member, while Fig. 8 summarises the distributions using violin plots. ~~As with precipitation, temperature extremes in the UKCP18-CPM dataset were evaluated by comparing the 95th (T_{95}) and 5th (T_5)~~

~~percentiles of daily mean temperature for the reference period with the HadUK-Grid dataset. Figure 7 and Figure 8 illustrate these comparisons using scatter plots (Figure 7) and violin plots (Figure 8).~~

~~The top panels of Figure 7 show scatter plots of T_{95} values from UKCP18-CPM against the corresponding observations from HadUK-Grid for each ensemble member, while the bottom panels present the same comparison for T_5 values.~~ For both T_{95} and T_5, the raw model outputs (light pink) show a fair level of correlation with the observations, with gradient values ranging from 0.97 to 1.1 and R^2 values between 0.84 and 0.91. This indicates reasonable agreement, but also some discrepancies, particularly in capturing the temperature extremes. After bias correction, the fitted slope and R^2 values for all four ensemble members are close to 1 in the reference period.~~the gradient and R^2 values for all four ensemble members improve to 1, indicating an almost perfect match between the corrected model outputs and the observed data.~~

Figure 8 complements this analysis by displaying violin plots of the distributions of T_{95} and T_5 for the observations (black), raw UKCP18-CPM (light pink), and bias-~~corrected~~ adjusted UKCP18-CPM (dark pink). The plots for T_{95} (left side) and T_5 (right side) clearly show that bias correction not only ~~corrects~~ adjusts the central tendencies of the temperature extremes but also adjusts their distribution.

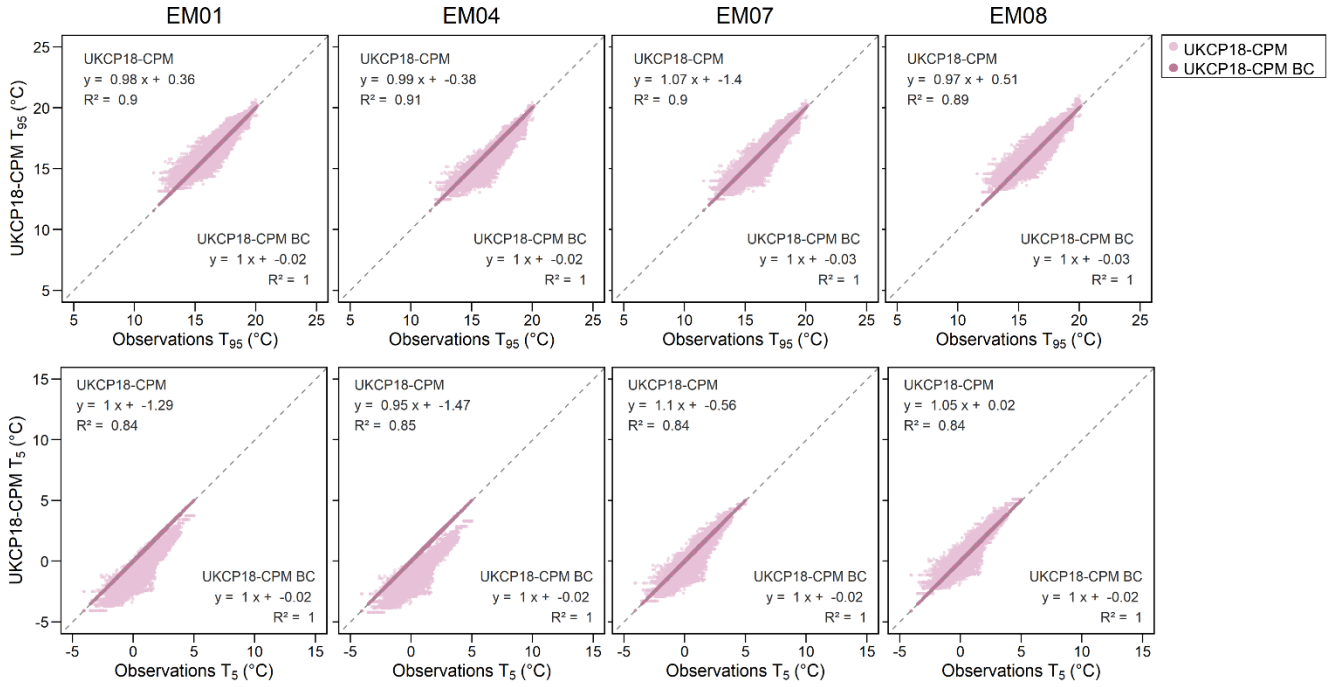

Figure 7: **The 95th (T_{95}, top row) and 5th (T_5, bottom row) percentile values of daily mean temperature for each ensemble member, plotted against HadUK-Grid (observations). Raw UKCP18-CPM (light pink) and bias-corrected UKCP18-CPM (dark pink) values are compared for the reference period.**~~**The 95th (T_{95}, top row) and 5th (T_5, bottom row) percentile values of daily mean temperature for each ensemble member, plotted against HadUK-Grid (observations). Raw UKCP18-CPM (light pink) and bias-corrected UKCP18-CPM BC (dark pink) values are compared for the reference period (December 1990 to November 2000).**~~

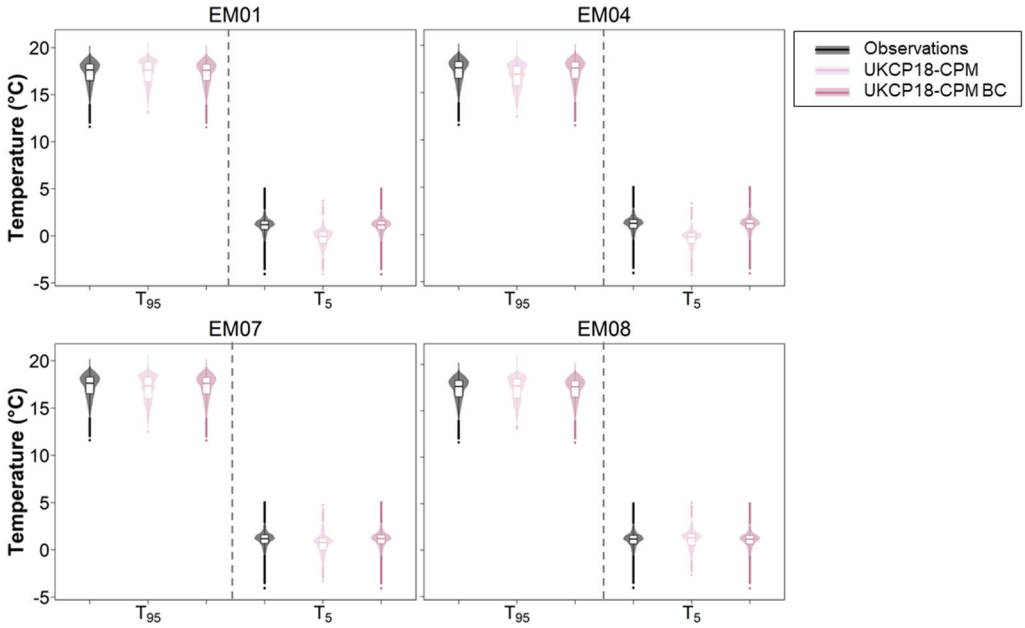

Figure 8: Violin plots of T_{95} and T_5 values for observations (HadUK-Grid, black), raw UKCP18-CPM (light pink), and bias-corrected UKCP18-CPM (dark pink) for each ensemble member during the reference period.~~Violin plots of T_{95} and T_5 values for observations (HadUK-Grid, black), raw UKCP18-CPM (light pink), and bias-corrected UKCP18-CPM-BC (dark pink) for each ensemble member during the reference period (December 1990 to November 2000).~~

3.3 Projected changes of bias-corrected UKCP18-CPM

Figure 9 and Figure 12a illustrate~~s~~ the projected percentage changes in hourly precipitation from bias-corrected UKCP18-CPM simulations, comparing future periods to baseline data (2030s in ~~Figure 9~~Figure 9a and 2070s in ~~Figure 9~~Figure 9b). The changes are presented for both annual maximum 1 h precipitation (Rx1h) and annual total precipitation (Ptot).~~the annual maximum (AMax) and annual total (AT) precipitation.~~

For the 2030s (Figure 9a and Figure 12a), the projections show an increase in Rx1h~~AMax~~ precipitation across all four ensemble members, with percentage changes ranging from approximately 19.9% (EM04) to 23.9% (EM08). Ptot also increases, but the changes are less pronounced, with values of 3% (EM08) and 9.4% (EM01).~~The changes in AT precipitation are also mostly positive but less pronounced, with increases ranging from 3% (EM08) to 9.4% (EM01).~~ This suggests increases can be disproportionally higher in the extreme precipitation events than in the annual totals. By the 2070s (Figure 9b and Figure 12a), the projected increase in Rx1h~~AMax~~ ~~precipitation~~ becomes even more pronounced, with percentage changes ranging from approximately 25.1% (EM07) to 39.1% (EM04), indicating a substantial intensification of maximum hourly precipitation. In contrast, the changes in Ptot~~AT~~ ~~precipitation~~ remain variable, with EM01 showing a decrease of 0.4%, confirming it as the driest member. EM04 and EM07 indicate wetter conditions, with increases of 8% and 6.1%, respectively, while EM08 shows a more moderate increase of 1.9%, representing a balanced response among the ensemble members.

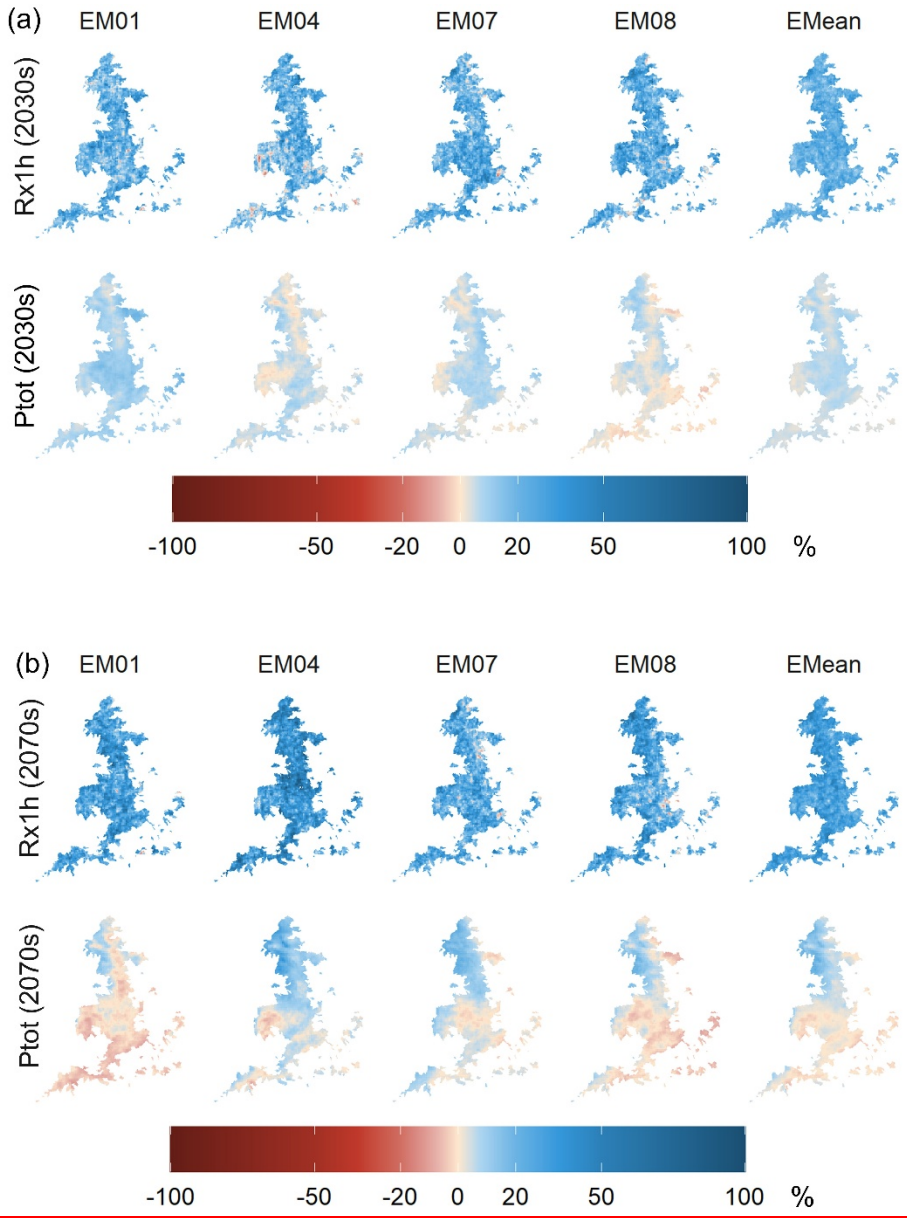
(a)
EM01
EM04
EM07
EM08
EMean
Rx1h (2030s)
Ptot (2030s)
-100
-50
-20
0
20
50
100
%
(b)
EM01
EM04
EM07
EM08
EMean
Rx1h (2070s)
Ptot (2070s)
-100
-50
-20
0
20
50
100
%

480

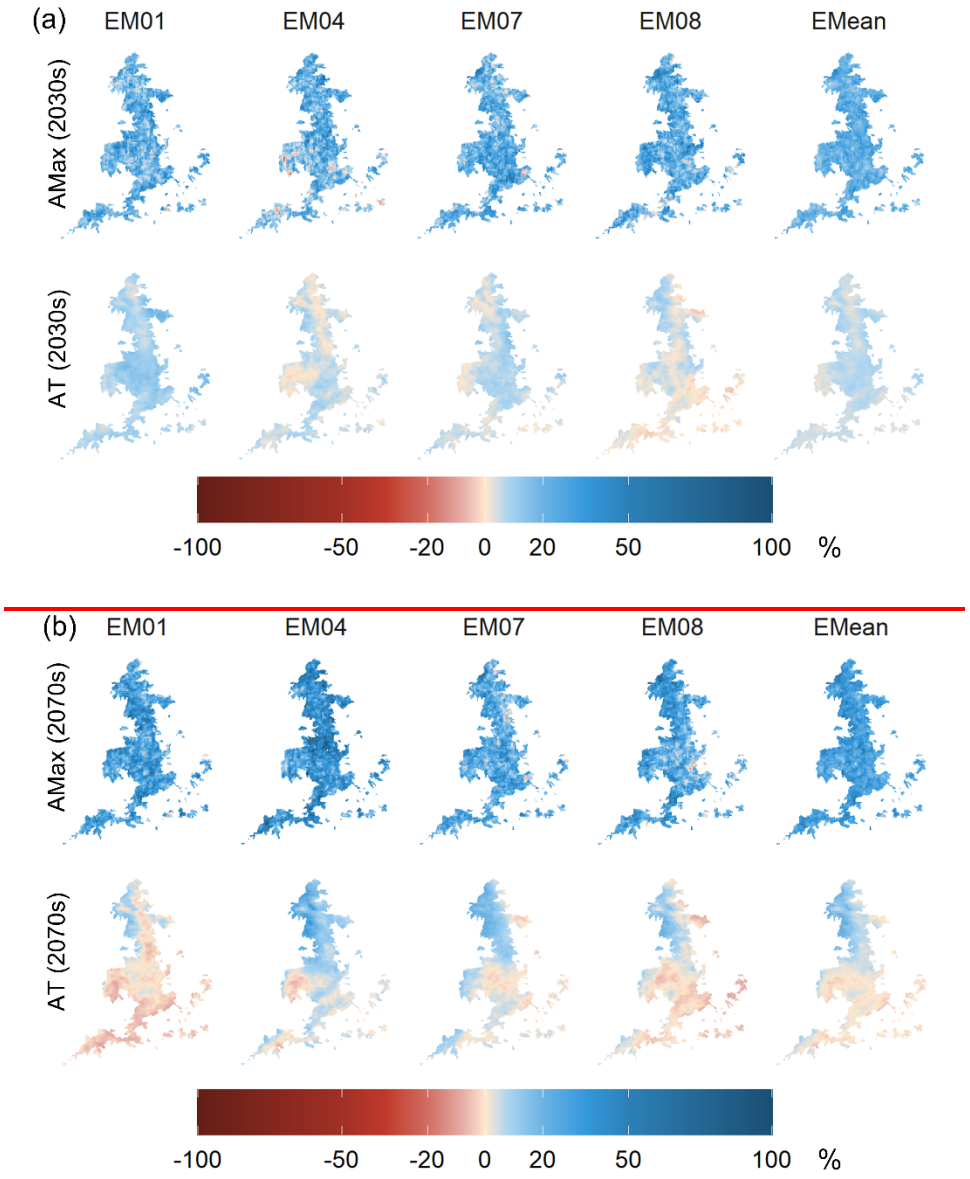

Figure 9: Projected percentage changes in annual maximum 1 h precipitation (Rx1h) and annual total precipitation (Ptot) from bias-corrected UKCP18-CPM simulations for the (a) 2030s and (b) 2070s, compared with the baseline period.~~Projected percentage changes in hourly precipitation from bias-corrected UKCP18-CPM simulations for the (a) 2030s and (b) 2070s, compared to the baseline period.~~

Figure 10 and~~ Figure 11~~ 12b illustrate the projected percentage changes in daily mean temperature from bias-corrected UKCP18-CPM simulations, comparing baseline period data to the future periods of the 2030s (~~Figure 10~~Figure 10) and the 2070s (~~Figure 11~~Figure 11). The projections are shown for annual maximum (Tmax), annual mean (Tmean), and annual minimum (Tmin)~~annual maximum (AMax), annual mean (AMean), and annual minimum (AMin)~~ temperatures.

For the 2030s (Figure 10 and Figure 12b), all four ensemble members project increases in Tmax~~AMax temperature~~, ranging from approximately 2.2 °C (EM01) to 3.2 °C (EM08). The Tmean~~AMean temperature~~ also shows consistent increases across ensemble members, with values ranging from 1.2 °C (EM07) to 1.7 °C (EM08). The Tmin~~AMin temperature~~ changes are also positive, ranging from 1.3 °C (EM07) to 2.2 °C (EM01), indicating an overall warming trend in the near future. By the 2070s (Figure 11 and Figure 12b), the increase in Tmax~~AMax~~ becomes more pronounced, with changes ranging from approximately 5 °C (EM01) to 6.5 °C (EM04), suggesting ~~a~~an intensification of maximum temperatures. Similarly, the Tm~~AM~~ean increases range from 3.1 °C (EM07) to 4.5 °C (EM04), and the Tm~~AM~~in changes range from 3.3 °C (EM07) to 4.7 °C (EM04). These results indicate substantial increases across ~~-~~all temperature metrics, i.e., maximum, mean, and minimum, by the 2070s. EM04 shows the highest level of warming in terms of Tm~~AM~~ean temperature, with an increase of 4.5 °C, followed by EM08 at 3.8 °C. In contrast, EM01 and EM07 show more moderate increases in Tm~~AM~~ean ~~temperature~~, with projected changes of 3.3 °C and 3.1 °C by the 2070s, respectively.

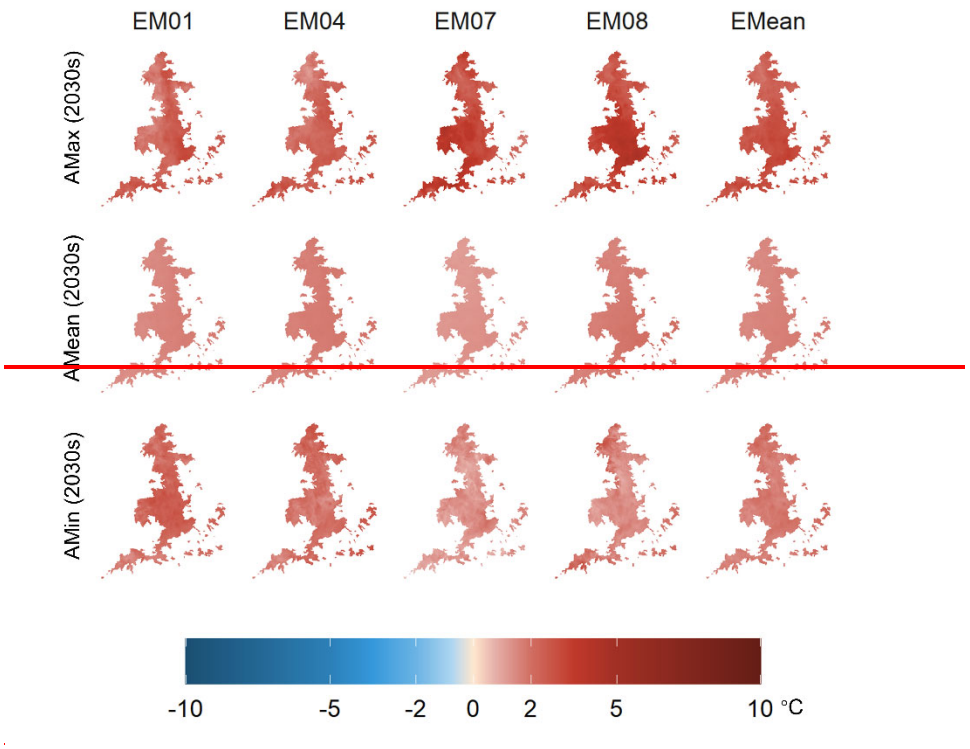

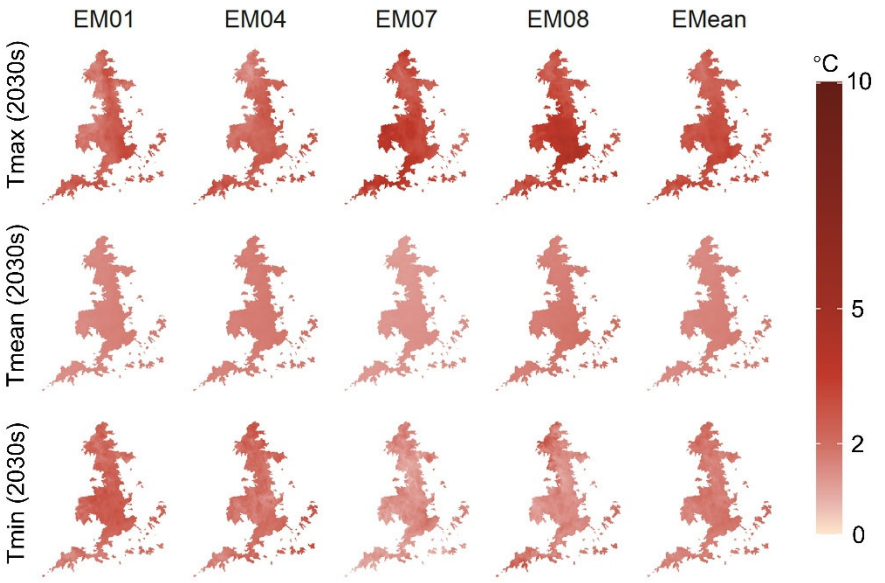

Figure 10: Projected changes (°C) in the annual maximum (Tmax), annual mean (Tmean), and annual minimum (Tmin) of daily mean temperature from bias-corrected UKCP18-CPM simulations. Results are shown for the 2030s relative to the baseline period, for each processed grid cell within the analysis mask. Columns show individual ensemble members (EM01, EM04, EM07, and EM08) and the ensemble mean (EMean). ~~Projected changes (°C) in daily mean temperature from bias-corrected UKCP18-CPM simulations for the 2030s, compared to the baseline period.~~

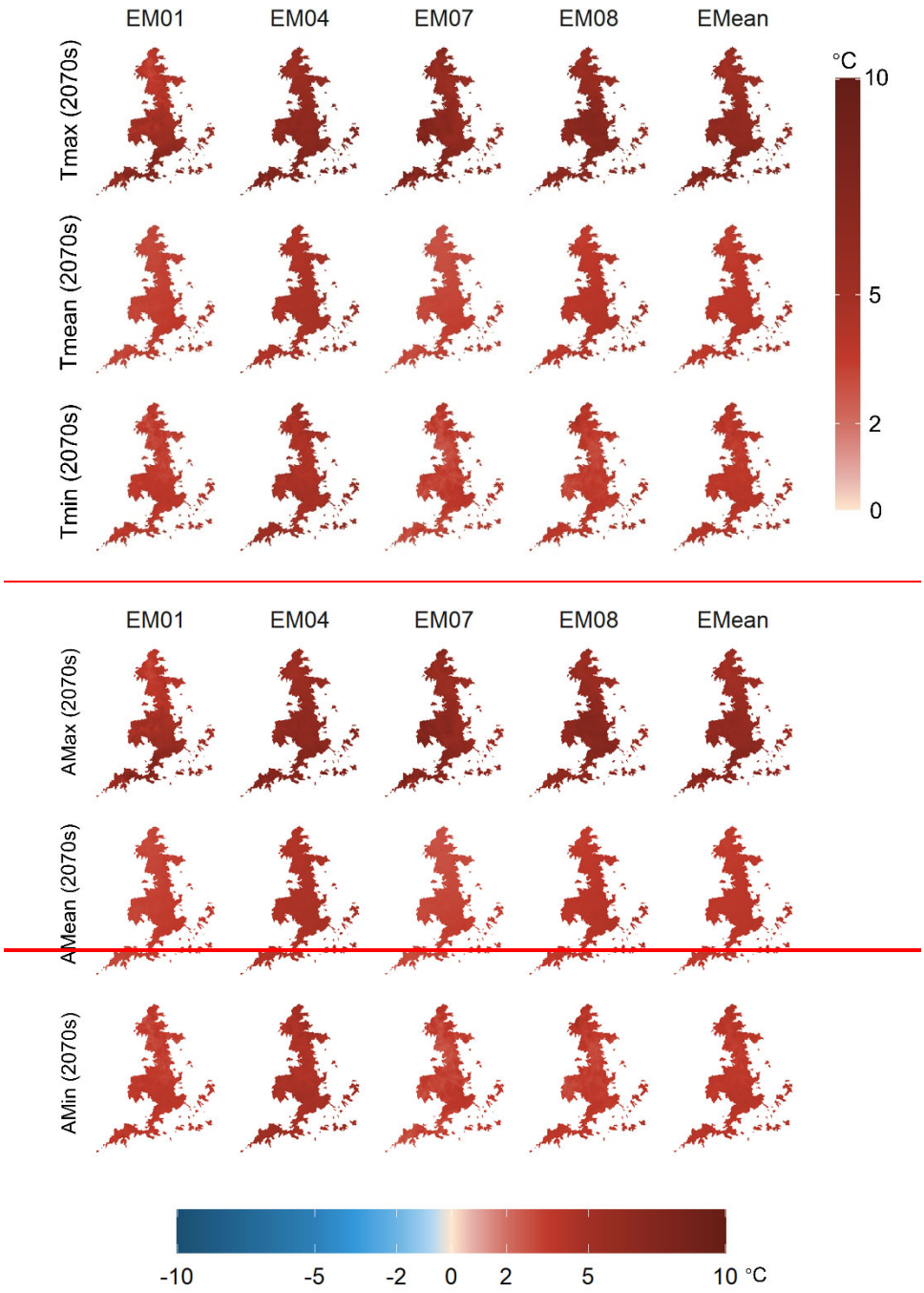

Figure 11: Projected changes (°C) in the annual maximum (Tmax), annual mean (Tmean), and annual minimum (Tmin) of daily mean temperature from bias-corrected UKCP18-CPM simulations. Results are shown for the 2070s relative to the baseline period, for each processed grid cell within the analysis mask. Columns show individual ensemble members (EM01, EM04, EM07, and EM08) and the ensemble mean (EMean). ~~Projected changes (°C) in daily mean temperature from bias-corrected UKCP18-CPM simulations for the 2070s, compared to the baseline period.~~

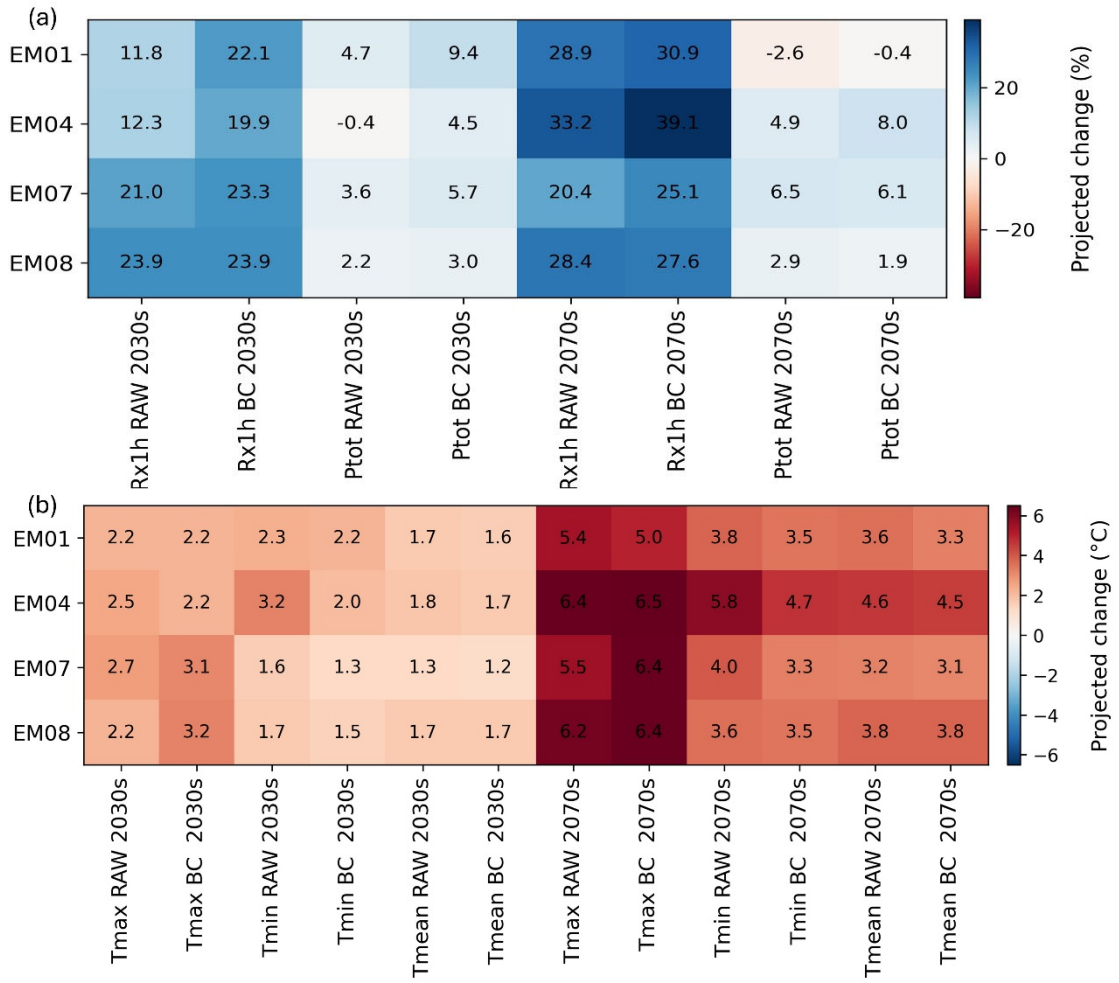

Figure 12: Projected changes in (a) annual maximum 1 h precipitation (Rx1h) and annual total precipitation (Ptot), and (b) annual maximum (Tmax), annual mean (Tmean), and annual minimum (Tmin) of daily mean temperature for UKCP18-CPM simulations before (RAW) and after bias correction (BC). Each value is the spatial average over the processed grid cells, shown for the 2030s and 2070s relative to the baseline period.

4 Discussion

This study provides a practical and reproducible bias correction approach for UKCP18-CPM hourly precipitation and daily mean temperature over England and evaluates how the adjusted outputs compare with observational reference datasets across mean behaviour, diurnal characteristics, and extremes. A set of bias-corrected 1 km UKCP18-CPM temperature and precipitation projections for England is provided, using empirical quantile mapping (QM) for daily mean temperature and diurnal bias correction (DBC) for hourly precipitation. The methodological contribution is not the development of a new bias-correction method, but the transparent implementation and assessment of established quantile-mapping methods for a

large CPM dataset at hourly resolution. This is relevant for impact applications where modelled rainfall timing and intensity can strongly influence simulated responses, especially for fast-response impact applications (e.g., short-duration rainfall-driven flooding). These results add evidence on the value of diurnal-cycle bias correction for sub-daily precipitation in convection-permitting simulations, a setting where such evaluations remain relatively limited. ~~presents a set of bias-corrected 1 km regional UK Climate Projections 2018 (UKCP18) Convection Permitting Model (CPM), focusing on temperature and precipitation projections for England, UK. By employing standard empirical quantile mapping bias correction method for daily mean temperature and diurnal bias correction method (DBC) for hourly precipitation, this study was able to effectively reduce systematic biases, resulting in model outputs that align closely with observational data. This bias-corrected dataset provides a more reliable basis for regional climate change analysis in England and demonstrates the value of these methods in improving high-resolution climate projections.~~

We applied empirical QM to daily mean temperature to address seasonal biases and distributional differences using a reproducible procedure. It is widely used because it can correct not only mean biases but also biases in variability and quantiles (Fang et al., 2015; Themeßl et al., 2011; Wilcke et al., 2013). For hourly precipitation, we used DBC by hour of day, because applying a single mapping across all hours can overlook systematic diurnal-cycle biases in sub-daily precipitation. Figure 5 supports this choice, showing that the bias-corrected ensemble more closely reproduces the observed hour-of-day pattern. This hour-of-day treatment is intended to reduce discrepancies that matter for sub-daily impact applications, consistent with the broader argument that correcting the diurnal cycle can improve sub-daily bias-correction strategies (Faghih et al., 2022). Therefore, we recommend using DBC for sub-daily variables. However, in this study we applied a 3 h moving window in the DBC. By incorporating hourly data from the previous and following hours, this may have contributed to some of the remaining discrepancies. It may be worth exploring whether omitting the moving window gives better results when the training period sample size is sufficiently large.

Before bias correction, the UKCP18-CPM simulations show considerable biases in both precipitation and temperature across various temporal and spatial scales. In general, UKCP18-CPM simulations show wet precipitation biases (especially in winter) and cool biases in temperature. These broad patterns are consistent with previous evaluations of UKCP18-RCM simulations (Reyniers et al., 2025) and the UKCP18-CPM science report (Kendon et al., 2019b). These residual biases are consistent with the broader CPM literature, which shows that although kilometre-scale models can improve the representation of precipitation compared with convection-parameterised RCMs, systematic biases and model uncertainty may remain, particularly for sub-daily precipitation and across different regional settings (Ban et al., 2021; Correa-Sánchez et al., 2025; Soares et al., 2024). After bias correction, both precipitation and temperature show substantially improved agreement with observations at monthly and diurnal timescales (Figs. 4 and 5). This suggests that bias correction provides a more reliable basis for downstream impact assessments than raw UKCP18-CPM output.~~Annual precipitation is generally overestimated by 4.6% to 18.3%, with more pronounced wet biases during winter (up to 43.5%) and significant spatial variability in summer, where precipitation is overestimated in the north and underestimated in the south (Figure 2). For temperature, there is a cooler bias across most ensemble members, with annual mean biases ranging from -0.87 °C to~~

~~0.02 °C (Figure 3). Furthermore, the diurnal cycle of precipitation (Figure 5) shows systematic overestimation, with the ensemble mean predicting consistently higher precipitation throughout the day compared to observations. After bias correction, substantial improvements are observed in both precipitation and temperature. Monthly precipitation and temperature closely match observed values (Figure 4). The diurnal cycle of precipitation is also improved, with the corrected ensemble mean accurately capturing both the variability and magnitude of observed precipitation across most hours of the day (Figure 5).~~

Future changes were also analysed for both precipitation and temperature in Figs. 9–12. In general, the bias-corrected projections indicate a clear intensification of annual maximum 1 h precipitation (Rx1h) by both the 2030s and 2070s, while changes in annual total precipitation (Ptot) remain smaller and spatially variable (Figs. 9 and 12). This pattern (i.e., stronger changes in short-duration extremes than in totals) is broadly consistent with CPM-based studies that report amplified changes for sub-daily extremes and a strong dependence on dynamical factors and regional setting (Dallan et al., 2024; Pichelli et al., 2021). The projected temperature changes are consistent with findings from the UKCP18-CPM science report (Kendon et al., 2019b), which indicated that mean temperature is expected to increase across all regions and seasons. Our findings also align well with existing literature, such as Robinson et al. (2023), who reported similar projected changes for UKCP18-RCM. This suggests that the bias-corrected projections remain broadly consistent with previously reported climate change signals.~~ In the 2030s, annual maximum precipitation is projected to increase across all ensemble members, suggesting a heightened intensity of extreme rainfall events, while the annual total precipitation changes are spatially variable. The projected temperature changes are consistent with findings from the UKCP18-CPM science report (Kendon et al., 2019b), which indicated that mean temperature is expected to increase across all regions and seasons. The results from our bias-corrected dataset similarly show increases in annual mean temperature, with ensemble member EM04 displaying the largest increase of up to 4.5 °C by the 2070s. By the 2070s, the trends for annual max precipitation become even more pronounced, with substantial intensification of maximum precipitation, and varying changes in annual totals ranging from slight decreases to moderate increases among different ensemble members. Notably, our findings regarding increased winter precipitation are also consistent with the UKCP Science report, which indicated obvious increases in winter precipitation, particularly due to more frequent wet days. These results reinforce the critical importance of considering a broad range of future scenarios to accurately account for potential climate impacts, which has been effectively captured using multiple ensemble members in our bias-corrected dataset.~~

Due to limitations in computational resources and time, we focused our analysis on four ensemble members: EM01, EM04, EM07, and EM08. These were selected to represent a diverse range of climate outcomes, from the driest to the wettest scenarios, allowing the bias-corrected dataset to effectively capture the range of possible climate responses in England. This sub-ensemble was chosen to balance computational efficiency with representativeness while ensuring that the selection captures a wide range of precipitation responses. The reduced number of ensemble members may influence the ensemble mean and spread compared to using all 12 members. Future studies could address this by expanding the bias correction to include more ensemble members and broader spatial coverage. Additionally, the integration of multivariate bias correction

methods (Cannon, 2018; Faghih et al., 2022) could offer the advantage of preserving inter-variable dependencies, ensuring that precipitation and temperature are corrected consistently without disrupting their natural relationship.~~Future studies involving the full ensemble could provide a more comprehensive assessment of ensemble spread and variability.~~

~~Our findings align well with existing literature, such as Robinson et al. (2023), who calculated the UKCP18-RCM projected changes and observed similar results. This supports the robustness of the bias correction methods and demonstrates their effectiveness in reducing uncertainties inherent in climate model projections. However, there are limitations to this approach. The analysis only covered four ensemble members and 62,488 grid points over 249 catchments in England, which may not fully capture the spatial and temporal variability across the entire UKCP18-CPM domain. Future studies could address this by expanding the bias correction to include more ensemble members and grid points, thereby improving the comprehensiveness and reliability of the climate projections. Additionally, the integration of multivariate bias correction methods (Cannon, 2018; Faghih et al., 2022) could offer the advantage of preserving inter variable dependencies, ensuring that precipitation and temperature are corrected consistently without disrupting their natural relationship.~~

This high-resolution bias-corrected dataset offers enhanced reliability, making it suitable for a wide range of climate change impact simulations and studies. The dataset's fine spatial and temporal resolution enables its application in various fields, such as flood forecasting, agricultural planning, and natural resource management, providing valuable insights for decision-making and long-term adaptation strategies. Future research could extend this analysis to other regions and incorporate additional climate models, providing a broader understanding of the impacts of climate change and helping to assess the applicability of these methods in different contexts. ~~Future research could extend this analysis to other regions and incorporating additional climate models that would provide a broader understanding of the impacts of climate change and help assess the applicability of these methods in various contexts.~~ This would not only improve the robustness of climate projections but also enhance the relevance and utility of bias-corrected datasets in informing climate adaptation strategies.

5 Conclusions

In this study, we applied bias correction to the UKCP18 Convection-Permitting Model (CPM) data to produce 1 km high-resolution precipitation and temperature projections for England, UK. Using quantile mapping (QM) as our bias correction method, we corrected biases in hourly precipitation and daily temperature data for four ensemble members (EM01, EM04, EM07, and EM08) selected to represent the spread of the full ensemble. Our results demonstrate that bias correction improved the alignment of UKCP18-CPM simulations with observational datasets, effectively reducing discrepancies (biases) and enhancing the model's performance across various metrics. The bias-corrected dataset provides a more reliable foundation for assessing future climatic changes and regional impacts across England. Although the bias-correction approaches applied here are established, this study provides new evidence of their performance for sub-daily precipitation in convection-permitting UK climate projections, including improvements in diurnal-cycle behaviour and sub-daily extremes relevant to impact modelling. The key findings are as follows:

1. Raw UKCP18-CPM simulations showed consistent wet biases for precipitation and cooler biases for temperature. For precipitation, the annual average biases ranged from 4.6% (EM07) to 18.3% (EM04), with the largest biases occurring in winter (DJF) ranging from 20.4% (EM01) to 43.5% (EM08). Temperature biases show a clear seasonal dependence, with winter (DJF) exhibiting larger spatial contrasts and summer (JJA) showing a more consistent cool bias across all members. On an annual mean basis, the temperature bias ranged from −0.87 °C (EM04) to +0.02 °C (EM08), with three of the four members showing a cool bias.~~For temperature, the annual mean bias ranged from -0.87 °C (EM04) to -0.42 °C (EM01), with a slight warm bias of 0.02 °C in EM08~~
2. After bias correction, both precipitation and temperature simulations aligned well with observational data. Monthly precipitation and temperature biases were substantially reduced, with bias corrected outputs closely following observed monthly patterns. The diurnal cycle of bias corrected precipitation captured the variability and magnitude of observed precipitation across most hours of the day. The 95th percentile (P_{95}) of hourly precipitation and temperature extremes (T_{95}) showed markedly improved agreement with observations after bias correction for both mean behaviour and high-percentile extremes (P_{95} and T_{95}).~~showed improved alignment with observational data. Monthly precipitation and temperature biases were substantially reduced, with corrected outputs closely following observed monthly patterns. The diurnal cycle of precipitation also showed marked improvement, with the corrected ensemble mean accurately capturing both the variability and magnitude of observed precipitation across most hours of the day. Furthermore, the 95th percentile (P_{95}) of hourly precipitation and temperature extremes (T95) demonstrated near-perfect agreement with observational datasets after correction, with R^2 values improving to 0.98 and 1.0, respectively.~~
3. Future projections for the 2030s and 2070s show significant increases in both precipitation and temperature. By the 2030s, annual maximum 1 h precipitation (Rx1h) ~~annual maximum precipitation (AMax)~~ is projected to increase by 19.9% (EM04) to 23.9% (EM08), while annual total precipitation (Ptot~~AT~~) shows more moderate increases, ranging from 3% (EM08) to 9.4% (EM01). In terms of temperature, annual mean temperature (~~AMean~~Tmean) increases range from 1.2 °C (EM07) to 1.7 °C (EM08) by the 2030s. By the 2070s, these trends become more pronounced, with Rx1h~~AMax precipitation~~ increasing by 25.1% (EM07) to 39.1% (EM04), and Tm~~AM~~ean ~~temperatures~~ projected to rise by 3.1 °C (EM07) to 4.5 °C (EM04). These projections indicate a potential for more intense extreme weather events, particularly for precipitation and temperature extremes, as the century progresses.

Appendix A

Table A1. NRFA ID of the selected 249 catchments

Catchment ID												
22006	27025	28003	28072	32008	37019	40004	43009	47014	52007	54011	55002	71006

22009	27026	28008	28074	33018	37020	40009	44001	47018	52009	54012	55013	71008
23001	27029	28009	28080	33019	37033	40011	44006	48003	52010	54016	55014	72002
23004	27030	28012	28081	33028	38007	40021	45001	48004	52011	54018	55018	72004
23008	27034	28018	28082	33031	38014	41001	45003	48005	52015	54019	68001	72007
23011	27035	28023	28085	33039	38018	41005	45004	48011	52016	54020	68003	72015
23016	27041	28024	28091	33058	39002	41006	45005	49001	53007	54027	68005	73005
24001	27042	28026	28093	34002	39005	41009	45009	49002	53008	54029	68020	73009
24004	27043	28031	28117	34005	39021	41011	45012	49004	53009	54034	69007	73010
24005	27047	28039	29003	34006	39034	41012	46003	50001	53017	54036	69012	73011
25001	27049	28040	30001	34007	39042	41013	46005	50002	53018	54038	69015	74001
25003	27051	28043	30004	34010	39052	41025	46008	50006	53023	54048	69017	74006
25020	27064	28046	30005	35008	39069	41027	46014	50007	53028	54049	69023	74007
26008	27071	28048	30011	36006	39087	41028	47001	50008	54001	54052	69027	75003
27001	27077	28052	30012	36011	39095	41029	47004	50011	54002	54057	69030	75004
27002	27080	28055	31010	36012	39099	42003	47005	51001	54004	54060	69032	75017
27003	27084	28056	31023	37008	39105	42017	47008	52004	54005	54063	69043	76007
27007	27089	28066	32003	37009	39143	43005	47009	52005	54007	54095	71001	76011
27021	27090	28067	32006	37018	39144	43007	47011	52006	54008	54096	71004	76014
101002	101005											

Data availability. The dataset is available at Zenodo (https://zenodo.org/records/16213003).

Author contributions. QZ performed most of the computational tasks and data curation. She performed most of the formal analysis and investigations and drafted the manuscript. NF assisted with writing bias correction program scripts. YH and TO provided guidance for the analysis and interpretation of the results. All authors reviewed the final manuscript and contributed to the writing.

Competing interests. The authors declare no competing financial or non-financial interests. One of the co-authors Yi He serves as an editor for Hydrology and Earth System Sciences (HESS).

Acknowledgements. The authors are grateful for the support provided by the high-performance Linux compute cluster at the University of East Anglia, which was used to conduct the bias correction in this study. We would also like to express our gratitude to Lukas Gudmundsson, the developer of the QM R package 'qmap,' for providing this valuable tool. Furthermore,

we thank the Met Office for making the HadUK-Grid and UKCP18-CPM datasets available, and the UK Centre for Ecology & Hydrology for access to the CEH-GEAR1hr dataset.

Financial support. This work was supported by the Open CLimate IMpacts modelling framework (OpenCLIM) project funded by the UK Natural Environment Research Council award number NE/T013931/1.

References

Ayugi, B., Tan, G., Ruoyun, N., Babaousmail, H., Ojara, M., Wido, H., Mumo, L., Ngoma, N. H., Nooni, I. K., and Ongoma, V.: Quantile Mapping Bias Correction on Rossby Centre Regional Climate Models for Precipitation Analysis over Kenya, East Africa, Water, 12, 801, https://doi.org/10.3390/w12030801, 2020.

Ban, N., Schmidli, J., and Schär, C.: Evaluation of the convection-resolving regional climate modeling approach in decade-long simulations, Journal of Geophysical Research: Atmospheres, 119, 7889–7907, https://doi.org/10.1002/2014JD021478, 2014.

Ban, N., Caillaud, C., Coppola, E., Pichelli, E., Sobolowski, S., Adinolfi, M., Ahrens, B., Alias, A., Anders, I., Bastin, S., Belušić, D., Berthou, S., Brisson, E., Cardoso, R. M., Chan, S. C., Christensen, O. B., Fernández, J., Fita, L., Frisius, T., Gašparac, G., Giorgi, F., Goergen, K., Haugen, J. E., Hodnebrog, Ø., Kartsios, S., Katragkou, E., Kendon, E. J., Keuler, K., Lavin-Gullon, A., Lenderink, G., Leutwyler, D., Lorenz, T., Maraun, D., Mercogliano, P., Milovac, J., Panitz, H.-J., Raffa, M., Remedio, A. R., Schär, C., Soares, P. M. M., Srnec, L., Steensen, B. M., Stocchi, P., Tölle, M. H., Truhetz, H., Vergara-Temprado, J., de Vries, H., Warrach-Sagi, K., Wulfmeyer, V., and Zander, M. J.: The first multi-model ensemble of regional climate simulations at kilometer-scale resolution, part I: evaluation of precipitation, Clim Dyn, 57, 275–302, https://doi.org/10.1007/s00382-021-05708-w, 2021.

Bannister, D., Orr, A., Jain, S. K., Holman, I. P., Momblanch, A., Phillips, T., Adeloye, A. J., Snapir, B., Waine, T. W., Hosking, J. S., and Allen-Sader, C.: Bias Correction of High-Resolution Regional Climate Model Precipitation Output Gives the Best Estimates of Precipitation in Himalayan Catchments, Journal of Geophysical Research: Atmospheres, 124, 14220–14239, https://doi.org/10.1029/2019JD030804, 2019.

Berthou, S., Kendon, E. J., Chan, S. C., Ban, N., Leutwyler, D., Schär, C., and Fosser, G.: Pan-European climate at convection-permitting scale: a model intercomparison study, Clim Dyn, 55, 35–59, https://doi.org/10.1007/s00382-018-4114-6, 2020.

Boé, J., Terray, L., Habets, F., and Martin, E.: Statistical and dynamical downscaling of the Seine basin climate for hydro-meteorological studies, International Journal of Climatology, 27, 1643–1655, https://doi.org/10.1002/joc.1602, 2007.

Breinl, K. and Di Baldassarre, G.: Space-time disaggregation of precipitation and temperature across different climates and spatial scales, Journal of Hydrology: Regional Studies, 21, 126–146, https://doi.org/10.1016/j.ejrh.2018.12.002, 2019.

Cannon, A. J.: Multivariate Quantile Mapping Bias Correction: An N-dimensional Probability Density Function Transform for Climate Model Simulations of Multiple Variables, Climate Dynamics, 50, 31–49, https://doi.org/10.1007/s00382-017-3580-6, 2018.

Cannon, A. J., Sobie, S. R., and Murdock, T. Q.: Bias Correction of GCM Precipitation by Quantile Mapping: How Well Do Methods Preserve Changes in Quantiles and Extremes?, J. Climate, 28, 6938–6959, https://doi.org/10/f7p6ft, 2015.

Chokkavarapu, N. and Mandla, V. R.: Comparative study of GCMs, RCMs, downscaling and hydrological models: a review toward future climate change impact estimation, SN Appl. Sci., 1, 1698, https://doi.org/10.1007/s42452-019-1764-x, 2019.

Correa-Sánchez, N., Dallan, E., Marra, F., Fosser, G., and Borga, M.: Orographic control on bias and uncertainty in extreme sub-daily precipitation simulations from a convection-permitting ensemble, Journal of Hydrology, 659, 133324, https://doi.org/10.1016/j.jhydrol.2025.133324, 2025.

Dai, A., Giorgi, F., and Trenberth, K. E.: Observed and model-simulated diurnal cycles of precipitation over the contiguous United States, J. Geophys. Res., 104, 6377–6402, https://doi.org/10.1029/98JD02720, 1999.

Dallan, E., Marra, F., Fosser, G., Marani, M., and Borga, M.: Dynamical Factors Heavily Modulate the Future Increase of Sub-Daily Extreme Precipitation in the Alpine-Mediterranean Region, Earth's Future, 12, e2024EF005185, https://doi.org/10.1029/2024EF005185, 2024.

Done, J., Davis, C. A., and Weisman, M.: The next generation of NWP: explicit forecasts of convection using the weather research and forecasting (WRF) model, Atmosph. Sci. Lett., 5, 110–117, https://doi.org/10.1002/asl.72, 2004.

Faghih, M., Brissette, F., and Sabeti, P.: Impact of correcting sub-daily climate model biases for hydrological studies, Hydrology and Earth System Sciences, 26, 1545–1563, https://doi.org/10.5194/hess-26-1545-2022, 2022.

Fang, G. H., Yang, J., Chen, Y. N., and Zammit, C.: Comparing bias correction methods in downscaling meteorological variables for a hydrologic impact study in an arid area in China, Hydrology and Earth System Sciences, 19, 2547–2559, https://doi.org/10.5194/hess-19-2547-2015, 2015.

Gudde, R., He, Y., Pasquier, U., Forstenhäusler, N., Noble, C., and Zha, Q.: Quantifying future changes of flood hazards within the Broadland catchment in the UK, Nat Hazards, 120, 9893–9915, https://doi.org/10.1007/s11069-024-06590-5, 2024.

Gudmundsson, L., Bremnes, J. B., Haugen, J. E., and Engen-Skaugen, T.: Technical Note: Downscaling RCM precipitation to the station scale using statistical transformations – a comparison of methods, Hydrol. Earth Syst. Sci., 16, 3383–3390, https://doi.org/10/f4drr9, 2012.

Gutmann, E., Pruitt, T., Clark, M. P., Brekke, L., Arnold, J. R., Raff, D. A., and Rasmussen, R. M.: An intercomparison of statistical downscaling methods used for water resource assessments in the United States, Water Resources Research, 50, 7167–7186, https://doi.org/10.1002/2014WR015559, 2014.

Hanlon, H. M., Bernie, D., Carigi, G., and Lowe, J. A.: Future changes to high impact weather in the UK, Climatic Change, 166, 50, https://doi.org/10.1007/s10584-021-03100-5, 2021.

Hannaford, J., Mackay, J. D., Ascott, M., Bell, V. A., Chitson, T., Cole, S., Counsell, C., Durant, M., Jackson, C. R., Kay, A. L., Lane, R. A., Mansour, M., Moore, R., Parry, S., Rudd, A. C., Simpson, M., Facer-Childs, K., Turner, S., Wallbank, J. R., Wells, S., and Wilcox, A.: The enhanced future Flows and Groundwater dataset: development and evaluation of nationally consistent hydrological projections based on UKCP18, Earth System Science Data, 15, 2391–2415, https://doi.org/10.5194/essd-15-2391-2023, 2023.

Hollis, D., McCarthy, M., Kendon, M., Legg, T., and Simpson, I.: HadUK-Grid—A new UK dataset of gridded climate observations, Geoscience Data Journal, 6, 151–159, https://doi.org/10.1002/gdj3.78, 2019.

IPCC: Climate Change 2021 – The Physical Science Basis: Working Group I Contribution to the Sixth Assessment Report of the Intergovernmental Panel on Climate Change, 1st ed., Cambridge University Press, https://doi.org/10.1017/9781009157896, 2023a.

IPCC: Climate Change 2022 – Impacts, Adaptation and Vulnerability: Working Group II Contribution to the Sixth Assessment Report of the Intergovernmental Panel on Climate Change, Cambridge University Press, Cambridge, https://doi.org/10.1017/9781009325844, 2023b.

Kay, A. and Brown, M.: Using sub-daily precipitation for grid-based hydrological modelling across Great Britain: Assessing model performance and comparing flood impacts under climate change, Journal of Hydrology: Regional Studies, 50, 101588, https://doi.org/10.1016/j.ejrh.2023.101588, 2023.

Kay, A., Bell, V. A., Davies, H. N., Lane, R. A., and Rudd, A. C.: The UKSCAPE-G2G river flow and soil moisture datasets: Grid-to-Grid model estimates for the UK for historical and potential future climates, Earth System Science Data, 15, 2533–2546, https://doi.org/10.5194/essd-15-2533-2023, 2023.

Keller, A. A., Garner, K. L., Rao, N., Knipping, E., and Thomas, J.: Downscaling approaches of climate change projections for watershed modeling: Review of theoretical and practical considerations, PLOS Water, 1, e0000046, https://doi.org/10.1371/journal.pwat.0000046, 2022.

Kendon, E. J., Jones, R. G., Kjellström, E., and Murphy, J. M.: Using and Designing GCM–RCM Ensemble Regional Climate Projections, J. Climate, 23, 6485–6503, https://doi.org/10.1175/2010JCLI3502.1, 2010.

Kendon, E. J., Stratton, R. A., Tucker, S., Marsham, J. H., Berthou, S., Rowell, D. P., and Senior, C. A.: Enhanced future changes in wet and dry extremes over Africa at convection-permitting scale, Nat Commun, 10, 1794, https://doi.org/10.1038/s41467-019-09776-9, 2019a.

Kendon, E. J., Fosser, G., Murphy, J., Chan, S., Clark, R., Harris, G., Lock, A., Lowe, J., Martin, G., Pirret, J., Roberts, N., Sanderson, M., and Tucker, S.: UKCP Convection-permitting model projections: Science report, 2019b.

Kendon, E. J., Short, C., Pope, J., Chan, S., Wilkinson, J., Tucker, S., Bett, P., and Harris, G.: Update to UKCP Local (2.2km) projections, Met Office Hadley Centre, Exeter, UK, 2021.

Kendon, E. J., Fischer, E. M., and Short, C. J.: Variability conceals emerging trend in 100yr projections of UK local hourly rainfall extremes, Nat Commun, 14, 1133, https://doi.org/10.1038/s41467-023-36499-9, 2023.

Kotlarski, S., Keuler, K., Christensen, O. B., Colette, A., Déqué, M., Gobiet, A., Goergen, K., Jacob, D., Lüthi, D., van Meijgaard, E., Nikulin, G., Schär, C., Teichmann, C., Vautard, R., Warrach-Sagi, K., and Wulfmeyer, V.: Regional climate modeling on European scales: a joint standard evaluation of the EURO-CORDEX RCM ensemble, Geoscientific Model Development, 7, 1297–1333, https://doi.org/10.5194/gmd-7-1297-2014, 2014.

Lafon, T., Dadson, S., Buys, G., and Prudhomme, C.: Bias correction of daily precipitation simulated by a regional climate model: a comparison of methods, International Journal of Climatology, 33, 1367–1381, https://doi.org/10.1002/joc.3518, 2013.

Lean, H. W., Clark, P. A., Dixon, M., Roberts, N. M., Fitch, A., Forbes, R., and Halliwell, C.: Characteristics of High-Resolution Versions of the Met Office Unified Model for Forecasting Convection over the United Kingdom, Mon. Wea. Rev., 136, 3408–3424, https://doi.org/10.1175/2008MWR2332.1, 2008.

Lewis, E., Quinn, N., Blenkinsop, S., Fowler, H. J., Freer, J., Tanguy, M., Hitt, O., Coxon, G., Bates, P., Woods, R., Fry, M., Chevuturi, A., Swain, O., and White, S. M.: Gridded estimates of hourly areal rainfall for Great Britain 1990-2016 [CEH-GEAR1hr] v2, 2022.

Maraun, D., Widmann, M., and Gutiérrez, J. M.: Statistical downscaling skill under present climate conditions: A synthesis of the VALUE perfect predictor experiment, International Journal of Climatology, 39, 3692–3703, https://doi.org/10.1002/joc.5877, 2019.

Maurer, V., Bischoff-Gauß, I., Kalthoff, N., Gantner, L., Roca, R., and Panitz, H.-J.: Initiation of deep convection in the Sahel in a convection-permitting climate simulation for northern Africa, Quarterly Journal of the Royal Meteorological Society, 143, 806–816, https://doi.org/10.1002/qj.2966, 2017.

Met Office, Hollis, D., McCarthy, M., Kendon, M., and Legg, T.: HadUK-Grid Gridded Climate Observations on a 1km grid over the UK, v1.1.0.0 (1836-2021), https://doi.org/10.5285/BBCA3267DC7D4219AF484976734C9527, 2022.

Met Office Hadley Centre: UKCP Local Projections on a 5km grid over the UK for 1980-2080, 2019.

Murata, A., Sasaki, H., Kawase, H., and Nosaka, M.: Evaluation of precipitation over an oceanic region of Japan in convection-permitting regional climate model simulations, Clim Dyn, 48, 1779–1792, https://doi.org/10.1007/s00382-016-3172-x, 2017.

Murphy, J. M., Harris, G. R., Sexton, D. M. H., Kendon, E. J., Bett, P. E., Clark, R. T., Eagle, K. E., Fosser, G., Fung, F., Lowe, J. A., McDonald, R. E., McInnes, R. N., McSweeney, C. F., Mitchell, J. F. B., Rostron, J. W., Thornton, H. E., Tucker, S., and Yamazaki, K.: UKCP18 Land Projections: Science Report, Met Office Hadley Centre, UK, 2018.

Ngai, S. T., Tangang, F., and Juneng, L.: Bias correction of global and regional simulated daily precipitation and surface mean temperature over Southeast Asia using quantile mapping method, Global and Planetary Change, 149, 79–90, https://doi.org/10.1016/j.gloplacha.2016.12.009, 2017.

Piani, C., Weedon, G. P., Best, M., Gomes, S. M., Viterbo, P., Hagemann, S., and Haerter, J. O.: Statistical bias correction of global simulated daily precipitation and temperature for the application of hydrological models, Journal of Hydrology, 395, 199–215, https://doi.org/10.1016/j.jhydrol.2010.10.024, 2010.

Pichelli, E., Coppola, E., Sobolowski, S., Ban, N., Giorgi, F., Stocchi, P., Alias, A., Belušić, D., Berthou, S., Caillaud, C., Cardoso, R. M., Chan, S., Christensen, O. B., Dobler, A., de Vries, H., Goergen, K., Kendon, E. J., Keuler, K., Lenderink, G., Lorenz, T., Mishra, A. N., Panitz, H.-J., Schär, C., Soares, P. M. M., Truhetz, H., and Vergara-Temprado, J.: The first multi-model ensemble of regional climate simulations at kilometer-scale resolution part 2: historical and future simulations of precipitation, Clim Dyn, 56, 3581–3602, https://doi.org/10.1007/s00382-021-05657-4, 2021.

Reiter, P., Gutjahr, O., Schefczyk, L., Heinemann, G., and Casper, M.: Does applying quantile mapping to subsamples improve the bias correction of daily precipitation?, International Journal of Climatology, 38, 1623–1633, https://doi.org/10.1002/joc.5283, 2018.

Reyniers, N., Osborn, T. J., Addor, N., and Darch, G.: Projected changes in droughts and extreme droughts in Great Britain strongly influenced by the choice of drought index, Hydrology and Earth System Sciences, 27, 1151–1171, https://doi.org/10.5194/hess-27-1151-2023, 2023.

Reyniers, N., Zha, Q., Addor, N., Osborn, T. J., Forstenhäusler, N., and He, Y.: Two sets of bias-corrected regional UK Climate Projections 2018 (UKCP18) of temperature, precipitation and potential evapotranspiration for Great Britain, Earth System Science Data, 17, 2113–2133, https://doi.org/10.5194/essd-17-2113-2025, 2025.

Riahi, K., Rao, S., Krey, V., Cho, C., Chirkov, V., Fischer, G., Kindermann, G., Nakicenovic, N., and Rafaj, P.: RCP 8.5—A scenario of comparatively high greenhouse gas emissions, Climatic Change, 109, 33, https://doi.org/10.1007/s10584-011-0149-y, 2011.

Roberts, N. M. and Lean, H. W.: Scale-Selective Verification of Rainfall Accumulations from High-Resolution Forecasts of Convective Events, Mon. Wea. Rev., 136, 78–97, https://doi.org/10.1175/2007MWR2123.1, 2008.

Robinson, E. L., Huntingford, C., Semeena, V. S., and Bullock, J. M.: CHESS-SCAPE: high-resolution future projections of multiple climate scenarios for the United Kingdom derived from downscaled United Kingdom Climate Projections 2018 regional climate model output, Earth System Science Data, 15, 5371–5401, https://doi.org/10.5194/essd-15-5371-2023, 2023.

Sangelantoni, L., Russo, A., and Gennaretti, F.: Impact of bias correction and downscaling through quantile mapping on simulated climate change signal: a case study over Central Italy, Theor Appl Climatol, 135, 725–740, https://doi.org/10.1007/s00704-018-2406-8, 2019.

Scaff, L., Prein, A. F., Li, Y., Liu, C., Rasmussen, R., and Ikeda, K.: Simulating the convective precipitation diurnal cycle in North America's current and future climate, Clim Dyn, 55, 369–382, https://doi.org/10.1007/s00382-019-04754-9, 2019.

Sexton, D. M. H., McSweeney, C. F., Rostron, J. W., Yamazaki, K., Booth, B. B. B., Murphy, J. M., Regayre, L., Johnson, J. S., and Karmalkar, A. V.: A perturbed parameter ensemble of HadGEM3-GC3.05 coupled model projections: part 1: selecting the parameter combinations, Clim Dyn, 56, 3395–3436, https://doi.org/10.1007/s00382-021-05709-9, 2021.

Shah, M., Thakkar, A., and Shastri, H.: Comparative analysis of bias correction techniques for future climate assessment using CMIP6 hydrological variables for the Indian subcontinent, Acta Geophys., 1–17, https://doi.org/10.1007/s11600-024-01378-4, 2024.

Smith, B. A., Birkinshaw, S. J., Lewis, E., McGrady, E., and Sayers, P.: Physically-based modelling of UK river flows under climate change, Frontiers in Water, 6, https://doi.org/10.3389/frwa.2024.1468855, 2025.

Soares, P. M. M., Careto, J. A. M., Cardoso, R. M., Goergen, K., Katragkou, E., Sobolowski, S., Coppola, E., Ban, N., Belušić, D., Berthou, S., Caillaud, C., Dobler, A., Hodnebrog, Ø., Kartsios, S., Lenderink, G., Lorenz, T., Milovac, J., Feldmann, H., Pichelli, E., Truhetz, H., Demory, M. E., de Vries, H., Warrach-Sagi, K., Keuler, K., Raffa, M., Tölle, M., Sieck, K., and Bastin, S.: The added value of km-scale simulations to describe temperature over complex orography: the CORDEX FPS-Convection multi-model ensemble runs over the Alps, Clim Dyn, 62, 4491–4514, https://doi.org/10.1007/s00382-022-06593-7, 2024.

Tabari, H., Paz, S. M., Buekenhout, D., and Willems, P.: Comparison of statistical downscaling methods for climate change impact analysis on precipitation-driven drought, Hydrology and Earth System Sciences, 25, 3493–3517, https://doi.org/10.5194/hess-25-3493-2021, 2021.

Tani, S. and Gobiet, A.: Quantile mapping for improving precipitation extremes from regional climate models, Journal of Agrometeorology, 21, 434–443, https://doi.org/10.54386/jam.v21i4.278, 2019.

Teutschbein, C. and Seibert, J.: Bias correction of regional climate model simulations for hydrological climate-change impact studies: Review and evaluation of different methods, Journal of Hydrology, 456–457, 12–29, https://doi.org/10.1016/j.jhydrol.2012.05.052, 2012.

Themeßl, M. J., Gobiet, A., and Leuprecht, A.: Empirical-statistical downscaling and error correction of daily precipitation from regional climate models, International Journal of Climatology, 31, 1530–1544, https://doi.org/10.1002/joc.2168, 2011.

Themeßl, M. J., Gobiet, A., and Heinrich, G.: Empirical-statistical downscaling and error correction of regional climate models and its impact on the climate change signal, Climatic Change, 112, 449–468, https://doi.org/10.1007/s10584-011-0224-4, 2012.

Thrasher, B., Maurer, E. P., McKellar, C., and Duffy, P. B.: Technical Note: Bias correcting climate model simulated daily temperature extremes with quantile mapping, Hydrology and Earth System Sciences, 16, 3309–3314, https://doi.org/10.5194/hess-16-3309-2012, 2012.

Trapp, R. J., Robinson, E. D., Baldwin, M. E., Diffenbaugh, N. S., and Schwedler, B. R. J.: Regional climate of hazardous convective weather through high-resolution dynamical downscaling, Clim Dyn, 37, 677–688, https://doi.org/10.1007/s00382-010-0826-y, 2011.

Vautard, R., Kadygrov, N., Iles, C., Boberg, F., Buonomo, E., Bülow, K., Coppola, E., Corre, L., van Meijgaard, E., Nogherotto, R., Sandstad, M., Schwingshackl, C., Somot, S., Aalbers, E., Christensen, O. B., Ciarlo, J. M., Demory, M.-E., Giorgi, F., Jacob, D., Jones, R. G., Keuler, K., Kjellström, E., Lenderink, G., Levavasseur, G., Nikulin, G., Sillmann, J., Solidoro, C., Sørland, S. L., Steger, C., Teichmann, C., Warrach-Sagi, K., and Wulfmeyer, V.: Evaluation of the Large EURO-CORDEX Regional Climate Model Ensemble, Journal of Geophysical Research: Atmospheres, 126, e2019JD032344, https://doi.org/10.1029/2019JD032344, 2021.

Vichot-Llano, A., Martinez-Castro, D., Giorgi, F., Bezanilla-Morlot, A., and Centella-Artola, A.: Comparison of GCM and RCM simulated precipitation and temperature over Central America and the Caribbean, Theor Appl Climatol, 143, 389–402, https://doi.org/10.1007/s00704-020-03400-3, 2020.

Weisman, M. L., Davis, C., Wang, W., Manning, K. W., and Klemp, J. B.: Experiences with 0–36-h Explicit Convective Forecasts with the WRF-ARW Model, Wea. Forecasting, 23, 407–437, https://doi.org/10.1175/2007WAF2007005.1, 2008.

Weusthoff, T., Ament, F., Arpagaus, M., and Rotach, M. W.: Assessing the Benefits of Convection-Permitting Models by Neighborhood Verification: Examples from MAP D-PHASE, Mon. Wea. Rev., 138, 3418–3433, https://doi.org/10.1175/2010MWR3380.1, 2010.

Wilcke, R. A. I., Mendlik, T., and Gobiet, A.: Multi-Variable Error Correction of Regional Climate Models, Climatic Change, 120, 871–887, https://doi.org/10.1007/s10584-013-0845-x, 2013.

Yun, Y., Liu, C., Luo, Y., Liang, X., Huang, L., Chen, F., and Rasmmusen, R.: Convection-permitting regional climate simulation of warm-season precipitation over Eastern China, Clim Dyn, 54, 1469–1489, https://doi.org/10.1007/s00382-019-05070-y, 2020.